



## Durham E-Theses

---

### *Noncovalent Control of $\beta$ -Cyclodextrin over Shapeshifting Molecules*

WEN, YUZHEN

#### How to cite:

---

WEN, YUZHEN (2020) *Noncovalent Control of  $\beta$ -Cyclodextrin over Shapeshifting Molecules*, Durham theses, Durham University. Available at Durham E-Theses Online: <http://etheses.dur.ac.uk/13717/>

#### Use policy

---

The full-text may be used and/or reproduced, and given to third parties in any format or medium, without prior permission or charge, for personal research or study, educational, or not-for-profit purposes provided that:

- a full bibliographic reference is made to the original source
- a [link](#) is made to the metadata record in Durham E-Theses
- the full-text is not changed in any way

The full-text must not be sold in any format or medium without the formal permission of the copyright holders.

Please consult the [full Durham E-Theses policy](#) for further details.



Durham  
University

Department of Chemistry

**Noncovalent Control of  $\beta$ -Cyclodextrin  
over Shapeshifting Molecules**

Yuzhen Wen

A Thesis Submitted for the Degree of Master by  
Research

*August 2020*

# Table of Contents

<b>Abstract</b>	i
<b>Acknowledgements</b>	ii
<b>Abbreviations</b>	iii
<b>Chapter 1</b>	
<b>1.1 Fluxional Carbon Cages</b>	1
<b>1.2 Cope Rearrangement</b>	1
<b>1.3 Bullvalene</b>	3
<b>1.4 Barbaralanes</b>	7
1.4.1 Synthesis of barbaralanes	8
<b>1.5 Application of Fluxional Carbon Cages</b>	12
<b>1.6 Project Aims</b>	16
<b>1.7 Results and Discussion</b>	17
<b>1.8 Conclusions and Future Work</b>	20
<b>1.9 Experimental</b>	20
1.9.1 General Methods	20
1.9.2 Synthetic Procedures	21
1.9.3 Failed Reactions	23
<b>1.10 Appendices</b>	26
<b>1.11 References</b>	27
<b>Chapter 2</b>	
<b>2.1 Chirality</b>	29
2.1.1 Dynamic Chirality	29
2.1.2 Noncovalent Control	31
<b>2.2 Cyclodextrin</b>	36
2.2.1 Stereoselectivity of Cyclodextrins	38
<b>2.3 Project Aims</b>	40
<b>2.4 Results and Discussion</b>	44
<b>2.5 Conclusions and Future Work</b>	46

<b>2.6 Experimental</b>	47
2.6.1 General Methods	47
2.6.2 Synthetic Procedures	47
2.6.3 Failed Reactions	48
<b>2.7 Appendices</b>	49
<b>2.8 References</b>	50

## Abstract

Fluxional carbon cages, such as bullvalene, barbaralane and the barbaralyl cation, exhibit their shapeshifting properties through the rapid Cope rearrangements which give thousands of degenerate isomers. When interacting with different guests through covalent modification or noncovalent bonding, the equilibrium distribution of isomers could be shifted, and this property can be utilized in molecular sensing. Barbaralanes only have two isomers, which makes it easier to control and investigate their dynamic equilibria. 9-Substituted barbaralanes, such as barbaralol, possess a dynamic  $sp^3$ -carbon stereocentre which is similar to an inverting nitrogen center.

This thesis involves two parts, the first part is synthesis of carbonyl derivative barbaralane. Barbaralane is an important building block for the synthesis and modification of various barbaralane derivatives. However, the modern synthetic route of barbaralane with gold(I) catalyst is expensive. We aim to integrate and optimize the traditional ways and expect to get large scale of barbaralane with a lower cost.

The second part is the noncovalent control over 9-substituted barbaralanes using  $\beta$ -cyclodextrin and its derivatives. Our hypothesis is that, after noncovalent control of  $\beta$ -CD, the equilibrium distribution of barbaralanes should be pushed towards one of the two stereoisomers. In the previous work of the group, after the tolyl barbaralol **2.19** was capsulated by  $\beta$ -CD, the complex appeared as a head-to-head dimer in solid state with one *R*- and one *S*- isomer in the two CD cavity. This kind of racemic self-sorting in a homochiral environment was unexpected. To further investigate this phenomenon, we aim to synthesize a  $\beta$ -CD dimer and use it to capsule **2.19** and observe its effect.

## Acknowledgements

Paul McGonigal. Thanks for the precious academic guidance and support over the last 11 months, the continuous care about our mental health during pandemic, the massive support for both my MSc and PhD application, the email on my birthday, but more importantly, the patience and confidence on me even when I am a complete idiot who messes everything up. Definitely one of the best and wisest people I have ever met, like an old father (even you are not old at all).

Fellas of CG235. Daily life in the office was always filled with laughter and joy thanks to these guys: Burhan Hussein, Promreet Saha, Andrew Turley, Phil Hope, Ho Chi Wong, Beth Beck.....I definitely enjoy hanging out and having drinks with you guys. Over the past year I have consumed more alcohol than the first 22 years of my life.

Aisha Bismillah. Thanks for the previous work you have done for this project: Synthesis of parent barbaralol **2.18** and tolyl barbaralol **2.19**, their NMR titration with cyclodextrin, and the crystal structure analysis of the binding complexes with  $\beta$ -CD (**Section 2.3**). Even you have left when I came here, I feel like you are always by my side. Thanks for tons of messages on Facebook about my research or life, which really makes me feel being cared of by a big sister.

Alyssa Avestro. Thanks for the unstoppable inspirations you bring to me and all others. You made me understand that the true feminism is to take responsibilities on our own initiative. Also, thanks for being another Take That fan by my side.

James Walton. Thanks for your cutest words and gestures (especially to my Pikachu) that make me laugh. You should call me when you visit Xi'an again.

Durham University and China Scholarship Council. Thanks for offering me the PhD funding after a tantalizing wait of 6 months and preventing me from leaving my unfinished masters project.

Andrew Sue. My final thank is to my old boss who made this all happen. Thanks for generously introducing me to Durham University, chatting with me about gossips on WeChat, and making me decide to walk on the path of academic in the future.

“In a moment of grace

A long leap of faith

There's still more glorious dawn awaits my life.”

## Abbreviations

Bu	Butyl
CD	Cyclodextrin
d	Doublet
DMF	Dimethylformamide
ESI	Electrospray ionisation
Et	Ethyl
HPLC	High Performance Liquid Chromatography
m	Multiplet
Me	Methyl
MS	Mass spectrometry
<i>m/z</i>	Mass to Charge Ratio
NBS	N-Bromosuccinimide
NMR	Nuclear magnetic resonance
Ph	Phenyl
q	Quartet
rt	Room temperature
s	Singlet
t	Triplet
TBS	<i>t</i> -Butyldimethylsilyl
TBSCl	<i>t</i> -Butyldimethylsilyl chloride
THF	Tetrahydrofuran
TLC	Thin-layer chromatography
TMS	Trimethylsilyl
UV	Ultraviolet
XRD	X-ray diffraction

# Chapter 1

## 1.1 Fluxional Carbon Cages

The term “fluxional carbon cages” refers to a series of chemical compounds such as bullvalene<sup>1</sup> (1.1), the barbaralyl cation<sup>2</sup> (1.2), barbaralane<sup>3</sup> (1.3) and semi-bullvalene<sup>4</sup> (1.4). They all have dynamic structures due to the rapid Cope rearrangements undergoing inside the molecules, which change the relative positions of atoms or functional groups and give thousands of degenerate isomers without breaking the carbon skeleton. For example, bullvalene has more than 1.2 million isomers and the barbaralyl cation has over 180 thousand isomers. (Figure 1.1)

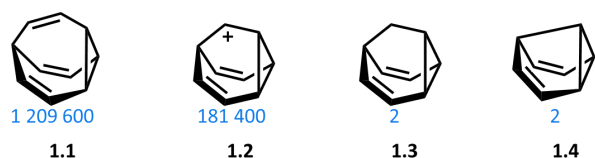


**Figure 1.1.** Structures of bullvalene (1.1), the barbaralyl cation (1.2), barbaralane (1.3) and semi-bullvalene (1.4) with the number of their degenerate isomers. (Figure reproduced from reference 33)

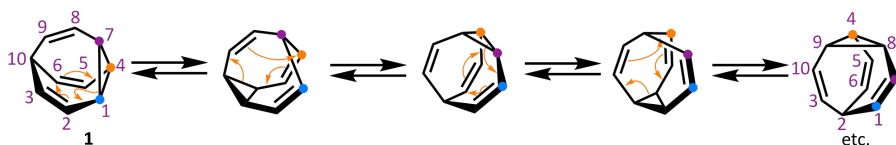
The existence of fluxional carbon cages has proven that a dynamic structural library can exist in a rigid molecule. They also have the potential to adapt their structures in response to the environment, making them potential building blocks for adaptive chemistry<sup>5</sup>. The properties of fluxional carbon cages have been investigated in both solution and solid state<sup>6</sup> and exploited as chemical sensors.

## 1.2 Cope Rearrangement

The Cope rearrangement, first developed by Arthur C. Cope,<sup>7</sup> is a rearrangement reaction which involves the [3,3]-sigmatropic rearrangement of 1,5-dienes. In this process, a  $\sigma$ -bonded atom or group flanked by one or more  $\pi$ -electron systems moves to a new location while the C-C bonds redistribute. Although the process is a pericyclic reaction, it can be assumed that the reaction undergoes a transition state with the same energy and structure as the diradical<sup>8</sup> even the diradical is not usually a true intermediate, and in stereochemistry, it appears to pass through a chair ring transition state.

In bullvalene and the barbaralyl cation (Scheme 1.1)<sup>33</sup>, the Cope rearrangement causes them to rapidly interconvert back and forth between thousands of constitutional isomers, which cannot be detected by nuclear magnetic resonance (NMR) in ambient temperature due to the Heisenberg Uncertainty Principle, and all the carbon and hydrogen signals appear equivalent on the NMR spectrum.

Amongst the bullvalene family, barbaralane and semibullvalene can only convert between two isomers because the olefin only exists on the two arms of the carbon cage. Thus, when the Cope rearrangement occurs and the  $\pi$  bond rearranges, each methine group maintains a substantially unchanged position. But in bullvalene, there is an additional olefin which opens the third arm of the carbon cage to the sigmatropic rearrangement. This additional approach allows each carbon to change its relative position with other carbons through a series of sequential sigmatropic rearrangements, resulting in thousands of degenerate isomers. Although the barbaralyl cation only has two olefins, the positive charge will generate a vacant p-orbital, and the electron density can shift to the vacant p-orbital, thereby promoting the third arm to participate in rearrangement and giving many more degenerate isomers. Overall, the number of degenerate isomers depends on the number of participating olefins and vacant p-orbitals in the carbon cage.



**Scheme 1.1.** Bullvalene (1) with five of its valence isomers demonstrated through Cope rearrangements. (Scheme reproduced from reference 33)

In unfunctionalized fluxional carbon cages, valence isomers are degenerate, i.e., they have equivalent constitutions. However, when one or more hydrogen atoms of the molecules are substituted with another group, the degeneracy can be changed, giving them shapeshifting properties. (Figure 1.2)<sup>33</sup>

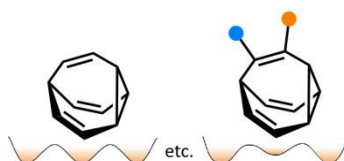


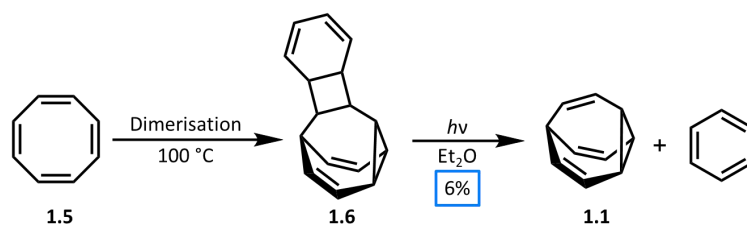
**Figure 1.2.** An unfunctionalised degenerate bullvalene vs functionalised nondegenerate bullvalene. (Figure

reproduced from reference 33)

### 1.3 Bullvalene

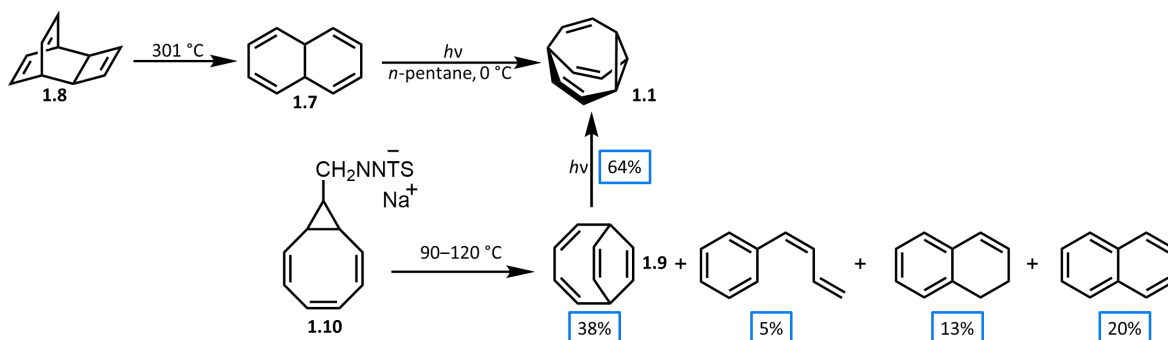
Bullvalene is a ten-carbon fluxional carbon cage with a three-fold axis of symmetry. Its structure was first predicted by Doering and Roth in 1963, elucidated by the sharp singlet in its NMR spectrum, they believed that “all ten carbon atoms must inevitably wander over the surface of a sphere in ever-changing relationship to each other”.<sup>1a</sup>

In the same year, Schröder produced bullvalene by photolysis of a dimer of cyclooctatetraene **1.5**, with benzene as the by-product.<sup>1b</sup> (Scheme 1.2)



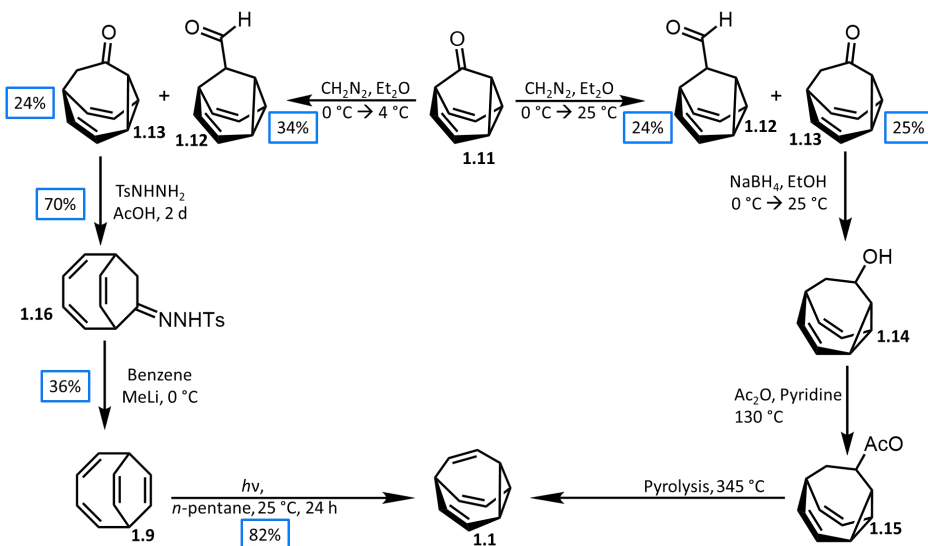
**Scheme 1.2.** The first synthesis of bullvalane (**1**) reported by Schröder.

Inspired by Schröder's route, Doering and Scott's team respectively managed to use the photolysis of other unsaturated alicyclic systems as the precursors to get higher yields of bullvalene<sup>9</sup> (Scheme 1.3): Doering and co-workers prepared bullvalene by irradiating 4a, 8a-dihydronaphthalene **1.7** and partial thermal decomposition of hydrocarbon at 0 °C in n-pentane. But the route is considered impractical because of the formation of naphthalene and other compounds that are difficult to separate from the desired bullvalene<sup>10</sup>. Scott and co-workers' route is relatively clean, which is based on irradiating bicyclo[4.2.2]deca-2,4,7,9-tetraene **1.9** to afford bullvalene. However, the transformation of tosylhydrazone sodium salt to bicyclo[4.2.2]deca-2,4,7,9-tetraene is low-yielding.



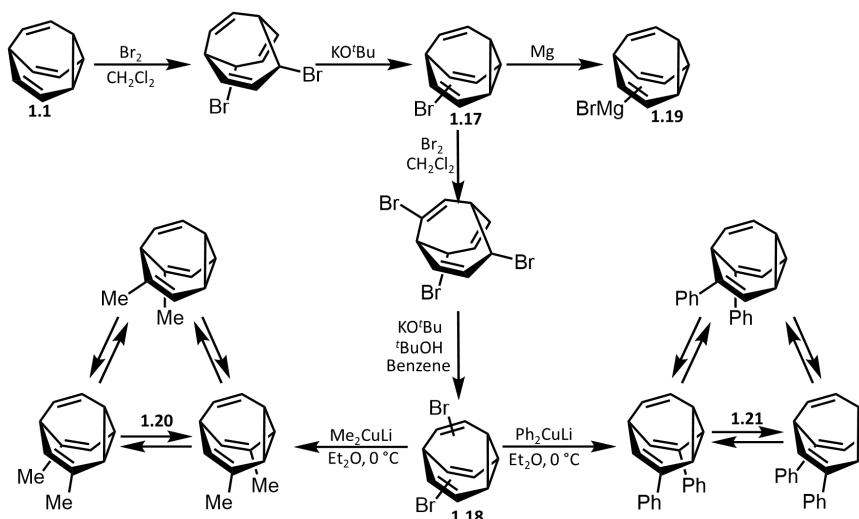
**Scheme 1.3.** Synthetic routes for bullvalene (**1.1**) reported by Doering and Scott.<sup>11,12</sup>

Doering and Serrotosa then developed different and longer synthetic routes (Scheme 1.4)<sup>33</sup>: first forming barbaralone, then going through different synthetic transformations to bullvalene. Doering's route starts with the treatment of barbaralone **1.11** with diazomethane in a one-carbon homologation to give bullvalone **1.13** and its isomeric aldehyde **1.12**. Reduction of bullvalone with sodium borohydride gives alcohol **1.14** which was then acetylated with acetic anhydride in pyridine at 130 °C. The final step is pyrolysis at 345 °C to get the desired bullvalene. Inspired by Doering's work, Serrotosa developed a similar route: it also goes through the formation of bullvalone and its isomeric aldehyde, then the bullvalone was treated with *p*-toluenesulphonyl hydrazine in acetic acid to give tosylhydrazone **1.16**. Anionic fragmentation with methyllithium in benzene at 0 °C and then conversion under UV irradiation leads to bullvalene in 82% yield.



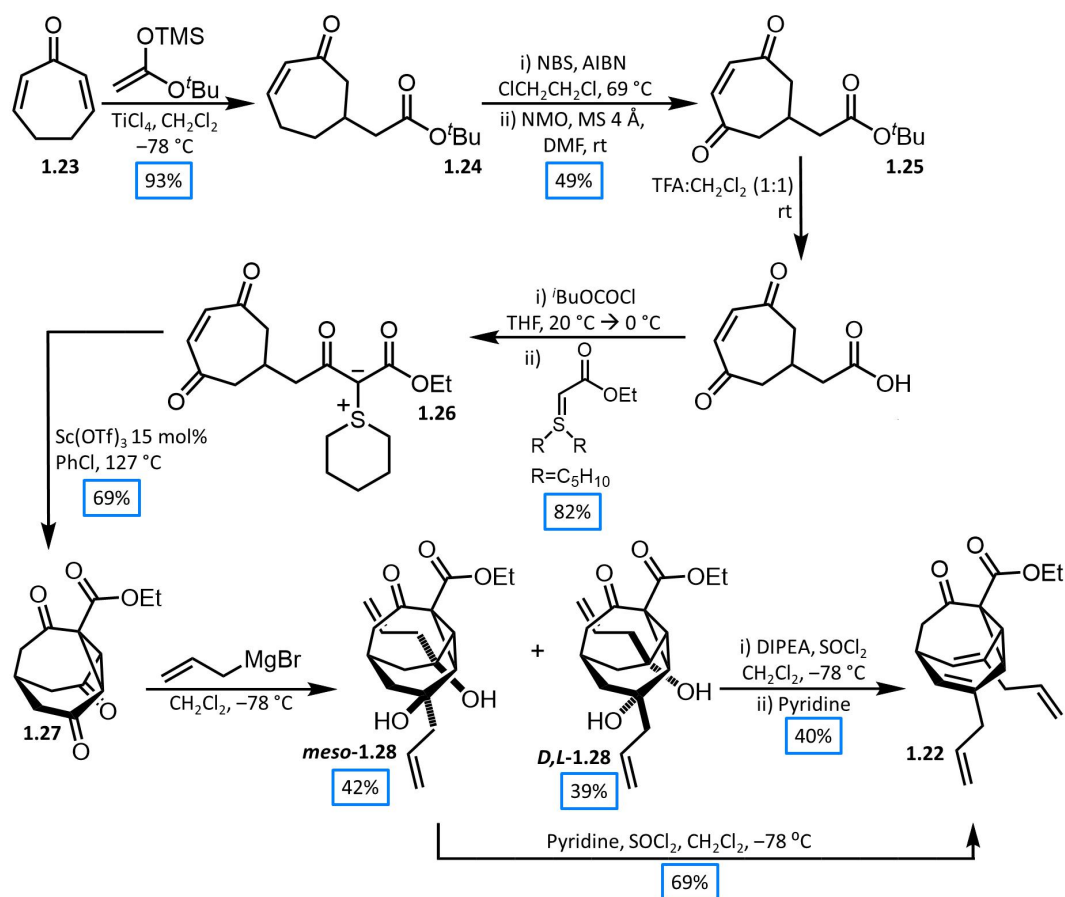
**Scheme 1.4.** Synthetic pathways towards bullvalene (**1.1**) produced by Doering and Serrotosa.<sup>11,12</sup> (Scheme reproduced from reference 33)

A series of mono- and poly-substituted bullvalene derivatives were then prepared by Schröder, Oth, and co-workers generally via the formation of the bromobullvalene<sup>13</sup> and dibromobullvalene<sup>14</sup> as intermediates. (Scheme 1.5) The bullvalene is first brominated with bromine and dehydrobrominated with potassium *tert*-butoxide to give bromobullvalene **1.17**, and this step is repeated to give dibromobullvalene **1.18**. Then several bullvalene derivatives, such as dimethylbullvalene and diphenylbullvalene, can be synthesized via these intermediates<sup>14a</sup>.



**Scheme 1.5.** Synthesis of bromobullvalene (**1.17**) and dibromobullvalene (**1.18**). (Scheme reproduced from reference 33)

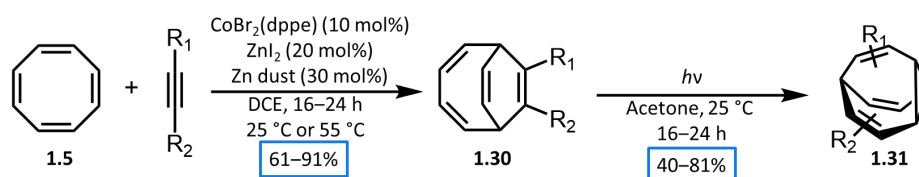
In 2006, a new synthetic pathway for tetra-substituted functionalised bullvalene **1.22** was developed by Bode and co-workers<sup>15</sup> (Scheme 1.6). It has been used in obtaining more elaborately-substituted bullvalenes, and investigations of their rearrangement and equilibrium properties. Bode's route starts with the Mukaiyama–Michael addition<sup>16</sup> of cycloheptadienone **1.23** to give the enone **1.24**, followed by radical bromination, oxidation with *N*-methylmorpholine-*N*-oxide, deprotection with trifluoroacetic acid and dichloromethane, then intramolecular cyclopropanation catalyzed by Lewis acid to give triketone **1.27**. From here, two of the carbonyl groups of the triketone were selectively added with allylmagnesium bromide to produce a 3:2 mixture of *meso*- and *D, L*-compound<sup>17</sup>. They can both be transformed into bullvalene **1.22** by the treatment of thionyl chloride and pyridine.



**Scheme 1.6.** Synthesis of the tetra-substituted functionalised bullvalene **1.22** reported by Bode and co-workers.

(Scheme reproduced from reference 33)

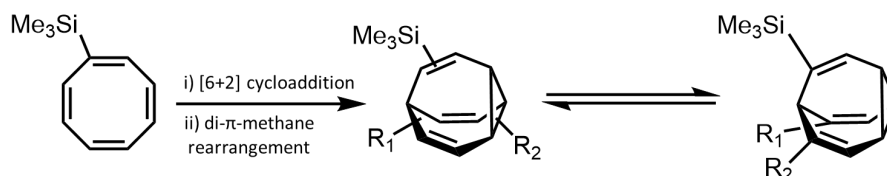
In the 2010s, metal-catalyzed cyclization has been used to get bullvalene derivatives. Au(I)-catalyzed and Co(I)-catalyzed reactions to prepare bullvalene precursors have been respectively reported by Echavarren and Fallon<sup>18</sup>. In Fallon's route, in the presence of  $\text{CoI}_2(\text{dppe})/\text{ZnI}_2/\text{Zn}$  catalyst, the cyclooctatetraene **1.5** undergoes a [6 + 2] cycloaddition with alkynes to produce the bicyclo[4.2.2]deca-2,4,7,9-tetraene intermediate **1.30**, then it undergoes a di- $\pi$ -methane photoisomerisation under UV irradiation to give the bullvalene derivatives **1.31** in the yield of 40 – 81%. (Scheme 1.7) This is by far the most efficient synthesis of bullvalene derivatives.



**Scheme 1.7.** The most concise synthesis of bullvalene (**1.1**) and its mono- and di-substituted analogues (**1.31**)

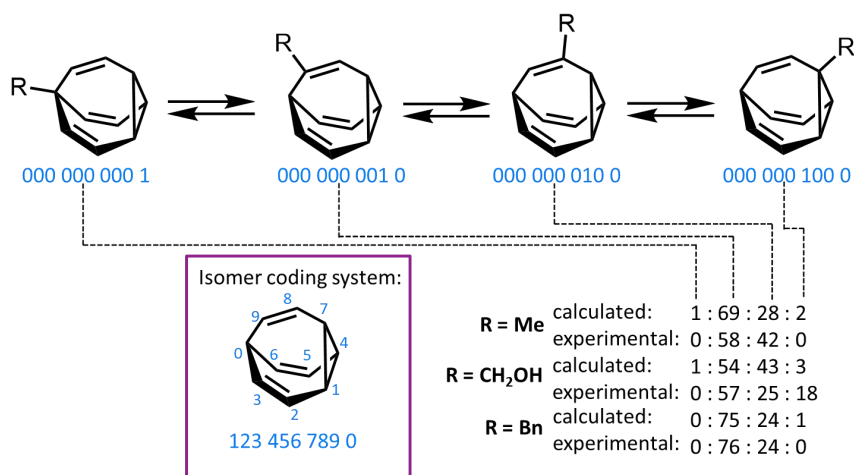
reported by Fallon and co-workers.

In 2019, based on the same principle, Fallon reported the synthesis of di- and tri-substituted bullvalenes through the [6 + 2] cycloaddition of trimethylsilyl-substituted cyclooctatetraenes,<sup>19</sup> including the first synthesis of heterogeneously trisubstituted bullvalenes. (Scheme 1.8)



**Scheme 1.8.** The synthetic route of di- and trisubstituted bullvalenes reported by Fallon.

To further investigate the structure library of bullvalenes and their substitution patterns, Bode developed an isomer coding system<sup>20</sup>. Every possible isomer is given with a ten-digit code in which the digit refers to the position of the carbon atom and the number represents the type of substituent. Based on this system, Fallon developed an algorithm which generates all possible bullvalene structures and their enantiomeric pairs as well as transition states to predict their equilibrium distribution. (Scheme 1.9) The algorithm's prediction of the isomer ratios for mono- and di-substituted bullvalene derivatives has been proven to be close to the modeling result, making it a valuable system when analyzing bullvalene mixtures.



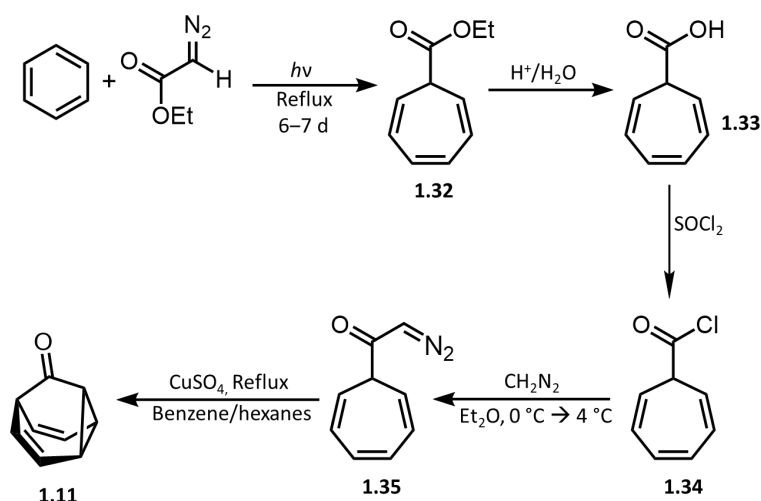
**Scheme 1.9.** Fallon's coding system for the mono-substituted bullvalene isomer network analysis. (Figure reproduced from reference 33)

## 1.4 Barbaralanes

Barbaralane is a rigid nine-carbon tricyclic diene. Compared to bullvalene, its ethylene arm is replaced by a methine group and it can only fluctuate between two degenerate isomers. Thus, the structures of barbaralanes are relatively easier to understand and their shapeshifting properties and equilibrium can be investigated as they are tractable systems.

### 1.4.1 Synthesis of barbaralanes

The first member of the barbaralane family reported was the carbonyl-containing derivative named barbaralone, which was prepared as an intermediate when Doering attempted to improve the synthesis of bullvalene in 1963.<sup>21</sup> The key step of the synthetic route is the insertion of an intramolecular carbene into the central double bond of the cycloheptatriene ring system, resulting in the formation of the carbonyl derivative. (Scheme 1.10) The route starts with the Buchner reaction of ethyl diazoacetate and benzene to obtain cycloheptatriene **1.32**.<sup>10</sup> The ester is hydrolyzed to carboxylic acid **1.33** and then converted to acid chloride **1.34** using thionyl chloride. Diazomethane is used to react with the acid chloride to give diazomethyl ketone **1.35**. Finally, the ketone is treated with copper (II) sulfate in the mixture of benzene and hexane under reflux to produce ketocarbene, which can form the barbaralone **1.11** in the intramolecular cyclopropanation reaction.

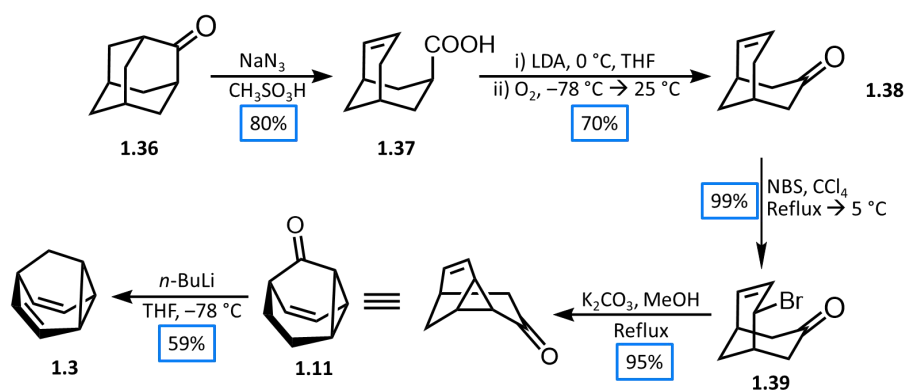


**Scheme 1.10.** Synthesis of barbaralone (**1.11**) reported by Doering and Roth.

Subsequently, a series of synthetic routes of barbaralone came to light.<sup>11,12</sup> Most of them take the

carbene insertion method as Doering's route, which uses diazomethane or trimethylsilyldiazomethane as the key reagent to form the diazomethyl ketone intermediate. The mixture is then heated at reflux with copper(II) source to give barbaralane.

In 1983, a completely different method to synthesize barbaralane was reported by Henkel<sup>3a</sup>: It starts with the treatment of 2-adamantanone **1.36** and sodium azide in methanesulfonic acid to give the carboxylic acid **1.37**. Oxidative decarboxylation of the carboxylic acid is obtained by treatment with lithium diisopropylamide, followed by oxidation and acidic post-treatment, giving the oxidized compound **1.38**. Then the allyl bromination reaction with *N*-bromosuccinimide (NBS) gives the bromoketone **1.39**, which participates in base-catalyzed ring closure to provide barbaralane **1.11**. Finally, by treatment with *n*-butyllithium in tetrahydrofuran, barbaralane is converted into tosyl forms to form barbaralane, eliminating the Bamford – Stevens type<sup>22</sup>. The overall yield is 59%. (Scheme 1.11)

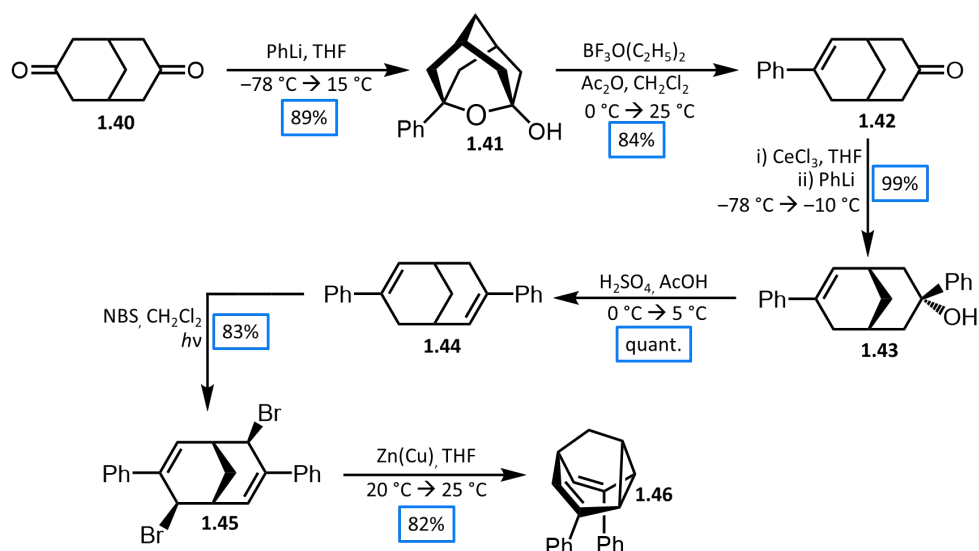


**Scheme 1.11.** Synthesis of barbaralane (**1.3**) from 2-adamantanone (**1.36**) reported by Henkel and co-workers.

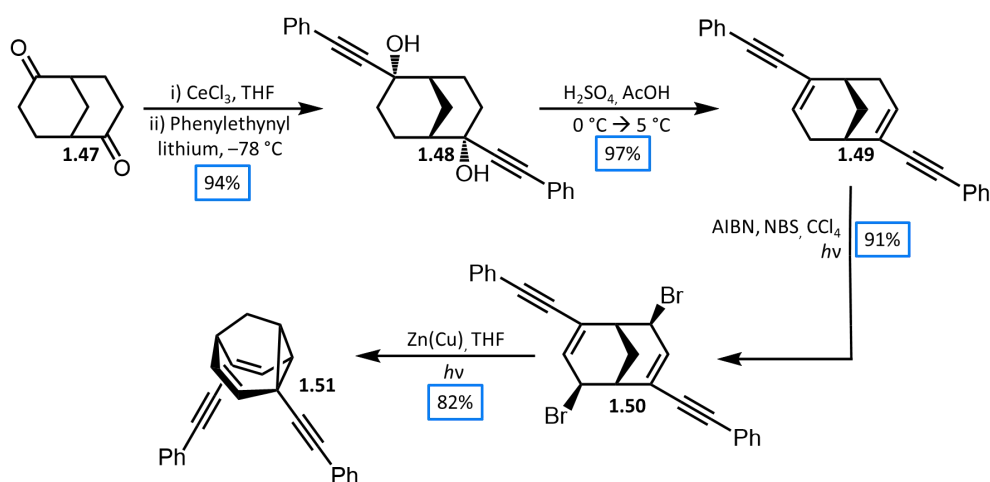
(Scheme reproduced from reference 33)

In 1995<sup>24</sup> and 1996<sup>26</sup>, Quast and co-workers developed two synthetic routes respectively for 3,7-substituted and 2,6-substituted barbaralanes **1.46** and **1.51** with various functions following a similar principle. The synthesis of **1.46** starts with bicyclo[3.3.1]nonanedione **1.40**, use phenyl lithium to give alcohol **1.41**, dehydration with sulfuric acid in acetic acid, allylic bromination with NBS, and cyclisation with a zinc-copper couple under irradiation. While **1.51** starts with bicyclo[3.3.1]nonane-2,6-dione **1.47** and use phenylethynyl lithium to give the alcohol **1.48**. The yield is 50% and 82%, respectively. The breakthrough of Quast's routes was to synthesize a series of substituted barbaralanes with different functions at different locations as well as an

improvement in the yield.<sup>25</sup> (Scheme 1.12<sup>33</sup> and 1.13<sup>33</sup>)



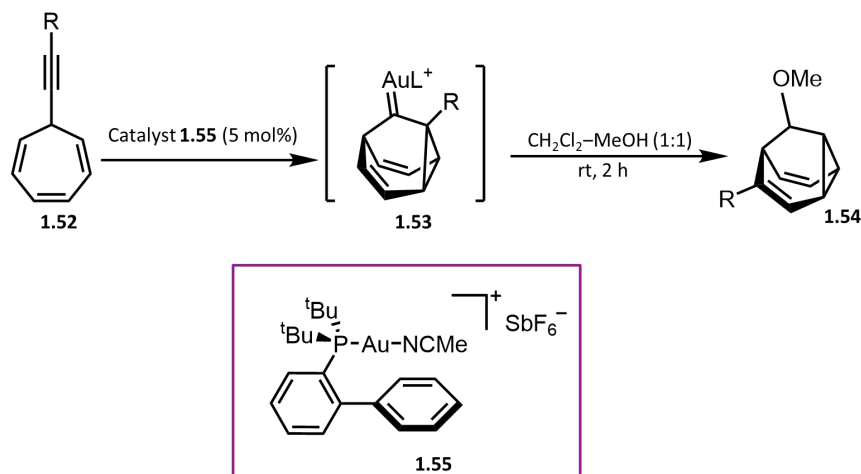
**Scheme 1.12.** Synthesis of 3,7-phenylbarbaralane (**1.46**) reported by Quast and co-workers. (Scheme reproduced from reference 33)



**Scheme 1.13.** Synthesis of 2,6-bis(phenylethynyl)barbaralane (**1.51**) developed by Quast and co-workers.

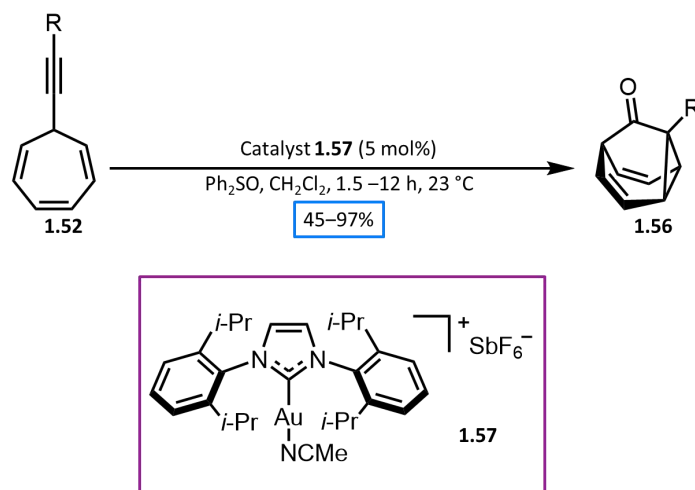
In recent years, cationic gold complexes have been used in the synthesis of barbaralanes for they can promote enyne cyclisations under mild conditions while exerting particular control over competitive reaction pathways, and stabilize intermediates with carbenoid character.<sup>27</sup> In 2012, Echavarren and co-workers investigated the cycloisomerisations of alkynyl cycloheptatrienes and the mechanism of the resulting indene formation by using different gold catalysts and  $\pi$ -Lewis acids<sup>27a</sup>: Alkynyl cycloheptatriene **1.52** is first prepared by nucleophilic addition of an acetylide to tropylium tetrafluoroborate, in the presence of a gold(I) catalyst, it cycloisomerises to a

gold-stabilised fluxional barbaralyl cation **1.53**. The barbaralyl cation will transform irreversibly to indenenes without nucleophiles, but if intercepted with an external nucleophile (such as methanol), the barbaralane methyl ether **1.54** can be isolated with only a small amount of indenyl by-products. The generation of the gold-stabilised barbaralyl cation has led to a short two-step pathway for synthesizing disubstituted barbaralane derivatives. (Scheme 1.14)<sup>33</sup>



**Scheme 1.14.** General procedure to synthesise substituted barbaralane methyl ethers (**1.54**) from alkynyl cycloheptatrienes (**1.52**). (Figure reproduced from reference 33)

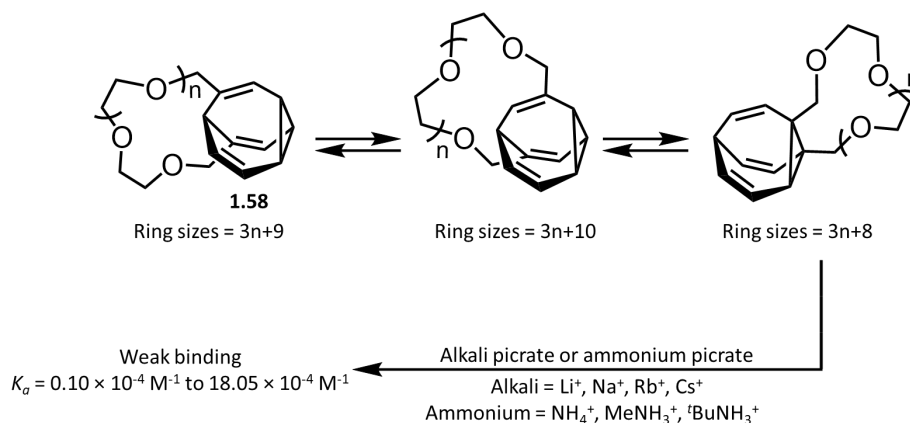
In 2016, Echavarren reported a simple two-step synthesis of barbaralone and its 1-substituted derivative, with the envision that oxidation of the barbaralyl intermediates could lead to substituted barbaralones<sup>27b</sup>. (Scheme 1.15) First activation and coordination to the alkyne triple bond occurs and this effectively promotes cyclization, followed by an attack of the external oxidant to provide  $\alpha$ -oxo gold (I) carbene, which is then oxidized in situ for intramolecular cyclopropane to give barbaralone. Several different gold(I) catalysts and oxidants were tested and finally diphenyl sulphoxide and (acetonitrile)[(2-biphenyl) di-tert-butylphosphine]gold(I) hexafluoroantimonate **1.57** were utilized. A series of substituted barbaralones **1.56** were successfully prepared via this synthetic route, with yields varying from 45% to 95%, and barbaralone itself reached a yield 97%. This is by far the simplest and most versatile pathway to prepare barbaralone.<sup>28</sup>



**Scheme 1.15.** General procedure to synthesize barbaralone (**1.11**) and substituted barbaralones (**1.56**) from substituted alkynyl cycloheptatrienes (**1.52**) developed by Echavarren and co-workers. (Scheme reproduced from reference 33)

## 1.5 Application of Fluxional Carbon Cages

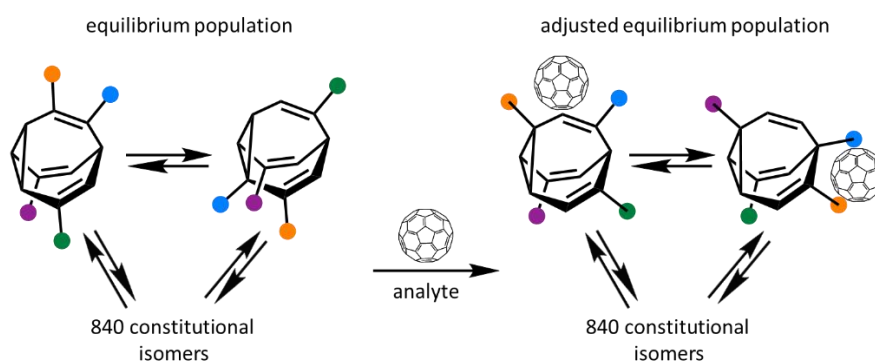
The first attempt to use bullvalene derivatives as adaptive shapeshifting mixtures was reported by Schröder and co-workers in 1979.<sup>29</sup> Inspired by the bullvalene principle conceived by Doering, they came up with the idea of “fluctuating or breathing rings”. They synthesized two crown ether-type compounds **1.58** with bullvalene as the linkage to investigate their association with metal-ion guests, which they expected to see the crown ether group to change ring size as the bullvalene interconverts via Cope rearrangements and lead to the selective binding of metal ions depending on different sizes. (Scheme 1.16)<sup>33</sup> However, only very weak associations were observed and the effect of metal ions on their equilibrium distribution could not be determined.



**Scheme 1.16.** Application of a crown-ether substituted bullvalene (**1.58**) with the binding of metal cations.

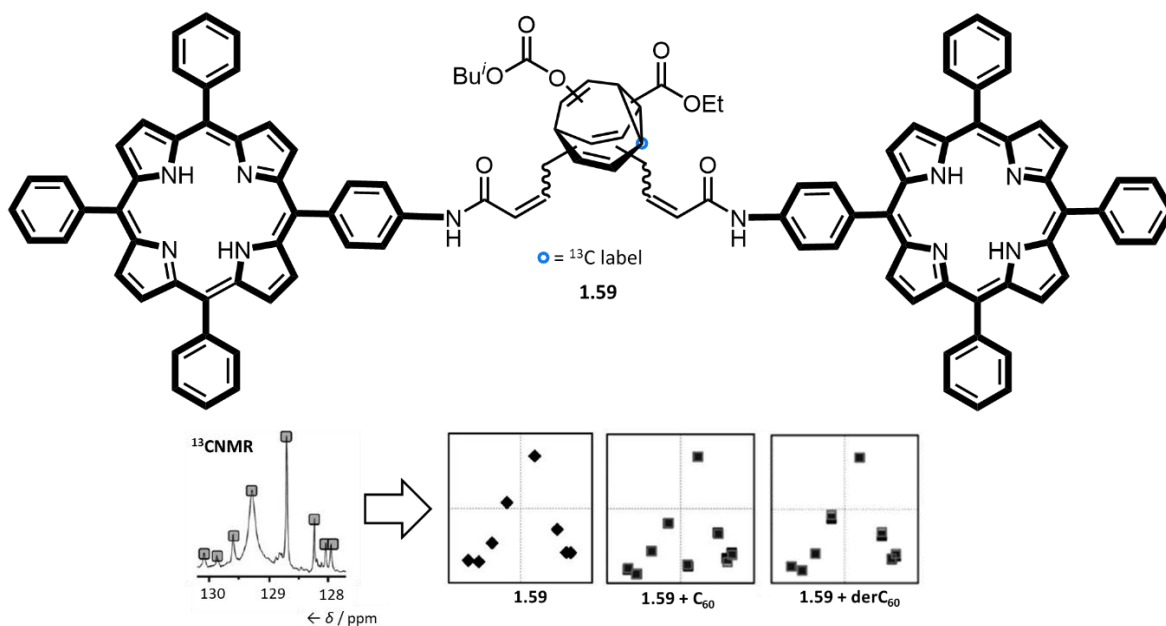
(Scheme reproduced from reference 33)

In 2009, Bode anticipated that the equilibrium distribution of oligo-substituted bullvalenes could be changed by interaction with fullerene analytes<sup>5a</sup>. Based on the high-affinity  $\pi$ - $\pi$  interactions of porphyrin with  $C_{60}$ , his group synthesized the bisporphyrin bullvalene and established the binding ability of a synthetic, shapeshifting molecular system. (Scheme 1.17)<sup>33</sup> The results showed that the addition of  $C_{60}$  shifts the equilibrium of bisporphyrin bullvalene towards isomers that more tightly bind with  $C_{60}$ , which demonstrated the possibility to spontaneously discover high-affinity binding complexes when interacted with a suitable guest.



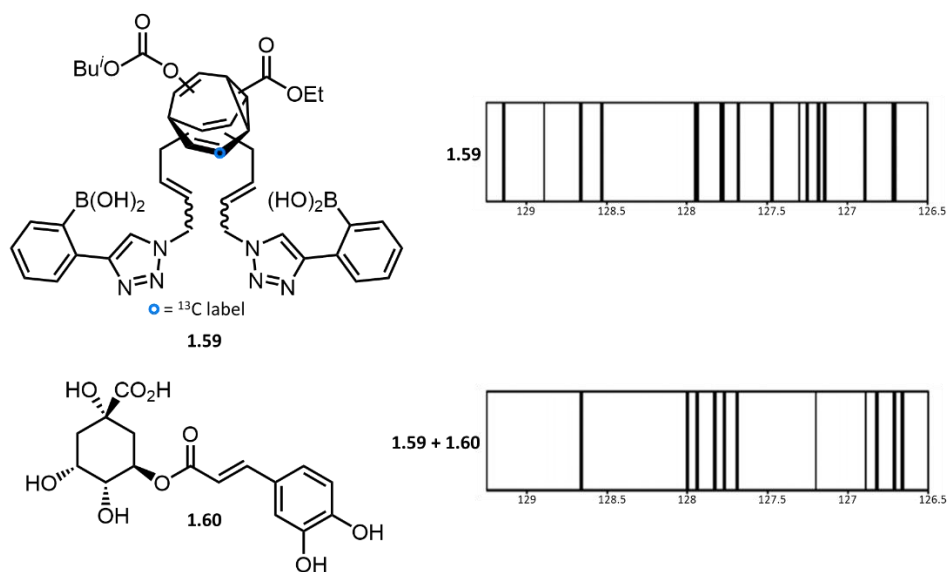
**Scheme 1.17.** The addition of a fullerene analyte alters the isomer distribution of the oligo-substituted bullvalene ( $C_{60}$  scaled down in size for illustrative purposes). (Figure reproduced from reference 33)

On this basis, the  $^{13}C$ -labelled bisporphyrin-bullvalene **1.59** was prepared by Bode and co-workers in 2012 to further investigate its application to the chemical sensing<sup>5b</sup>. (Scheme 1.18)<sup>33</sup> By comparing the  $^{13}C$ -NMR spectra of fullerene derivatives without analytes and those treated with fullerene  $C_{70}$ , they proved that the bullvalene core could easily distinguish very similar analytes.



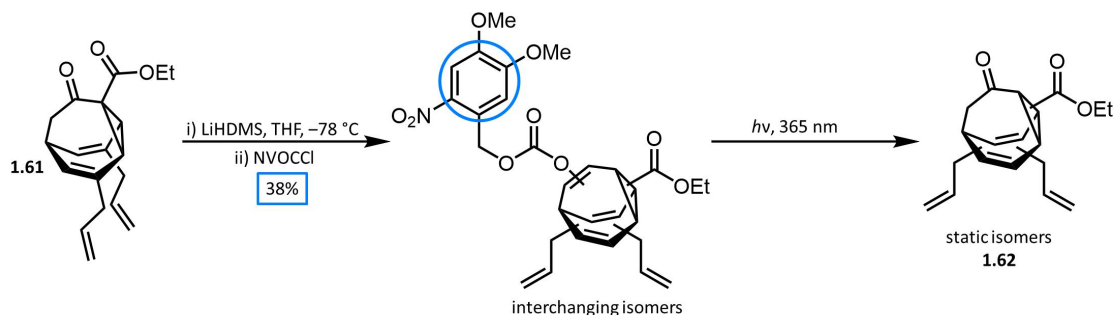
**Scheme 1.18.**  $^{13}\text{C}$ -labelled bisporphyrin-bullvalene (**1.59**) and a graphical representation of its  $^{13}\text{C}$  NMR spectrum converted to its corresponding peak pattern showing the equilibrium population. (Figure reproduced from reference 33)

In 2013, Bode and co-workers reported the first case of analyte binding through covalent bonding.<sup>30</sup> By attaching boronic acid end groups, they prepared the bullvalene derivative **1.59** which could interact with and sense polyols through dynamic covalent condensation reactions, developing a dynamic bis-boronic acid-based sensor array **1.60** which could detect different polyols, and the  $^{13}\text{C}$ -NMR signals were transformed into easy-to-read barcodes. (Scheme 1.19)<sup>33</sup> The results showed that the barcode in the presence of every different polyol was distinctive, which demonstrated that the bullvalene sensor is readily able to distinguish different polyols with closely related structures. Compare to the classic sensor arrays, one of its significant advantages is that the selectivity of a specific scope would not be reduced due to the dominance of the strongest binding analyte.



**Scheme 1.19.**  $^{13}\text{C}$ -labelled bis-boronic acid bullvalene (**1.59**) and its barcode compared to the barcode of a mixture of **1.59** and **1.60**. (Figure reproduced from reference 33)

Bode also prepared a bullvalene derivative with a photolabile carbonate substituent **1.62** in 2010<sup>19a</sup>, which proved that photolysis of the *o*-nitroveratryloxycarbonate (NVOC) bisallyl bullvalene halts the Cope rearrangements, thus the addition of a suitable photocleavable group could block the fluxional behaviour and isolate the adapted structures. (Scheme 1.20)



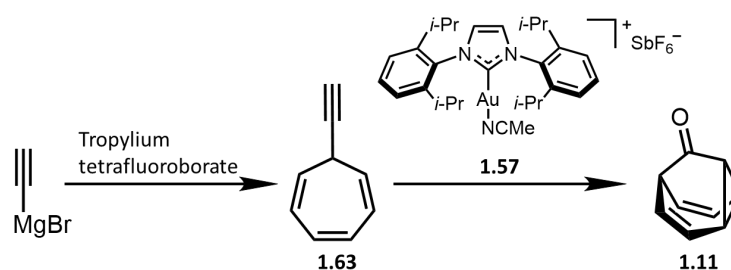
**Scheme 1.20.** Synthesis and photolysis of NVOC bisallyl bullvalene (**1.62**). (Scheme reproduced from reference 33)

The shapeshifting sensors' ability to differentiate similar analytes could be a promising feature. Currently, the main shortcoming is that the difference between  $^{13}\text{C}$ -NMR could be minor and difficult to be recognized. This problem could be solved by improving the molecular design, such as the development of systems with shorter and more rigid functional handles. Complementary spectroscopic techniques may also be focused on. Improvements of these sensors can lead to their

sensing of more complex molecules, making them more appealing in the future.

## 1.6 Project Aims

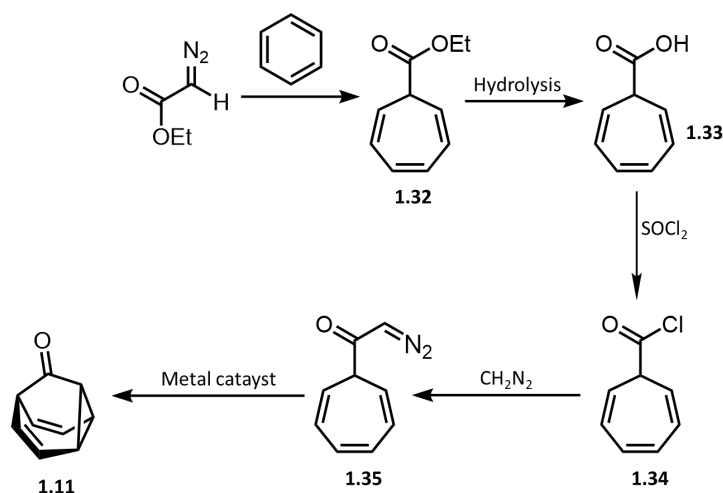
The project aims are to integrate the synthetic routes for barbaralone **1.11** and attempt to scale up the barbaralone obtained each time. Barbaralone is an important intermediate in the synthesis of barbaralane and its derivatives. Currently the simplest and fastest route to make barbaralone is reported by Echavarren in 2016, which consists of cyclization of alkynyl cycloheptatriene **1.63** and then oxidation via gold(I) catalyst **1.57** and diphenyl sulphoxide (Scheme 1.21). However, when attempted practically, only a small amount of barbaralone could be obtained each time (100 – 200 mg) because the catalyst **1.57** and tropylium tetrafluoroborate starting material are both very expensive, and the intermediate **1.63** is highly volatile, which makes the further synthesis and modification slower and more costly.



**Scheme 1.21.** Gold(I)-catalysed synthesis of barbaralone **1.11**

In contrast, the earliest synthetic route reported by Doering and Roth is an alternative way to achieve a larger scale synthesis of barbaralone, where the reagents are relatively low-costing and the product of every step is relatively stable. It involves five steps: the Buchner reaction of ethyl diazoacetate and benzene; hydrolysis of ester **1.32**; conversion of the carboxylic acid **1.33** into the acid chloride **1.34** with thionyl chloride; followed by the reaction with diazomethane to give diazomethyl ketone **1.35**; and finally the treatment of ketone with copper (II) sulfate to give ketocarbene, which then forms the barbaralone **1.11** in the intramolecular cyclopropanation.

In this project, Doering and Roth's route will be utilized to synthesize a much larger scale of barbaralone. The steps will be improved in this process, including the reaction conditions of ester hydrolysis and the choice of metal catalyst in the last step. (Scheme 1.22)

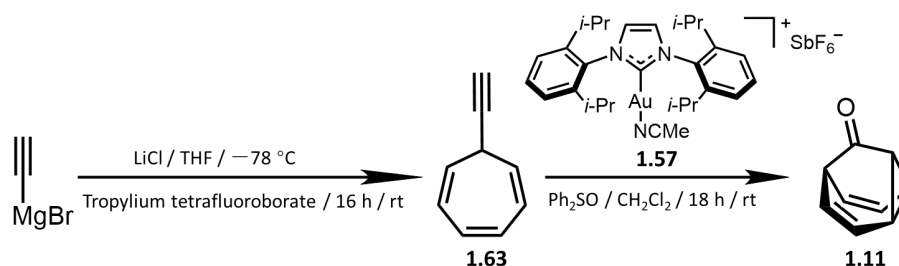


**Scheme 1.22.** Planned route of making **1.11** following Doering and Roth's report.

## 1.7 Results and Discussion

### Two-step synthesis of barbaralone **1.11** via gold(I) catalyst

Barbaralone was first obtained through the modern two-step method reported by Echavarren to isolate a sample for analytical comparison. Ethynyl magnesium bromide was treated with dry LiCl and tropylium tetrafluoroborate to get the intermediate **1.63**, which is highly volatile and should only be eluted by n-pentane in the column chromatography, then **1.63** was converted to barbaralone **1.11** with diphenyl sulfoxide and the gold(I) catalyst **1.57** in 24% yield. (Scheme 1.23) Due to its shapeshifting properties, the  $^1\text{H-NMR}$  spectrum of **1.11** only shows three broad peaks.

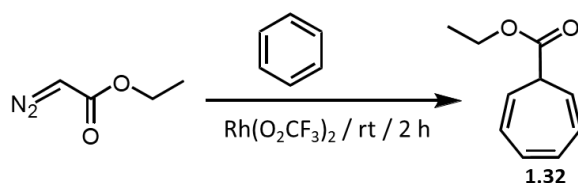


**Scheme 1.23.** Synthetic scheme of **1.11** following the modern method.

### Synthesis of ethyl cyclohepta-2,4,6-triene-1-carboxylate **1.32**

Synthesis of **1.32** was achieved through the Buchner reaction of ethyl diazoacetate and benzene,

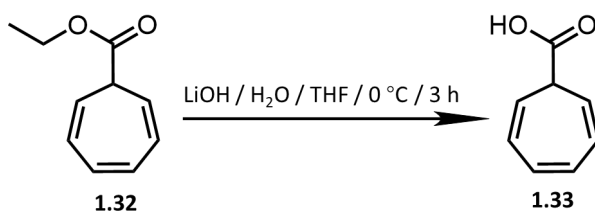
following the procedure optimized by Teyssié and co-workers in 1980.<sup>31</sup> Rhodium(II) trifluoroacetate dimer was used to stabilize the carbene and form the seven-member ring (Scheme 1.24). The reaction was easily completed by adding the ethyl diazoacetate into the stirred mixture of 0.02 mol%  $\text{Rh}(\text{O}_2\text{CF}_3)_2$  and benzene with the use of an automated syringe pump and no further purification was required. **1.32** was obtained in a yield of 86% after removing the excess benzene under reduced pressure. Due to the toxicity of benzene, it was removed by distillation in the fumehood.



**Scheme 1.24.** Synthetic scheme of **1.32**.

### Synthesis of cyclohepta-2,4,6-triene-1-carboxylic acid **1.33**

The hydrolysis of the ester **1.32** initially followed the procedure reported by Streitwieser,<sup>32</sup> which treats **1.32** with  $\text{NaHCO}_3$  under reflux, however, it did not work in practice: The  $^1\text{H-NMR}$  indicated that isomerization of the cycloheptatriene ring occurred, suggesting that the reaction conditions were too strong. Due to these results, a series of bases and acids were attempted under different temperatures. The results showed that some conditions were too strong and also led to isomerization whereas others were too mild to break the ester bond. The conditions which proved to be successful were  $\text{LiOH}$  at  $0^\circ\text{C}$  (Scheme 1.25). The product **1.33** was obtained in 66% yield.



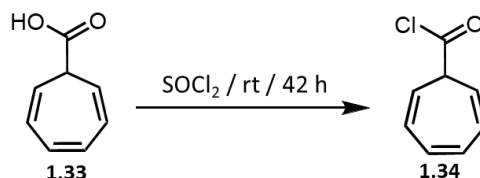
**Failed conditions:**

- 1)  $\text{NaHCO}_3 / \text{MeOH} / \text{H}_2\text{O} / 60^\circ\text{C} / 2 \text{ h}$
- 2)  $\text{KOH} / \text{MeOH} / 35^\circ\text{C} / 1 \text{ h}$
- 3)  $\text{KOH} / \text{THF} / \text{H}_2\text{O} / 60^\circ\text{C} / 2 \text{ h}$
- 4) Acid / THF /  $\text{H}_2\text{O}$  / Gradient temperature

**Scheme 1.25.** Synthetic scheme of **1.33** and the failed conditions.

### Synthesis of cyclohepta-2,4,6-triene-1-carbonyl chloride **1.34**

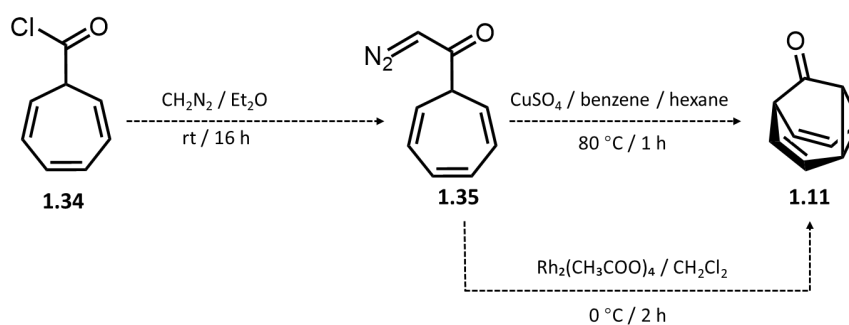
The conversion of acid **1.33** into acid chloride **1.34** was simply achieved in 88% yield by stirring the mixture of thionyl chloride and **1.33** for 42 h under room temperature (Scheme 1.26). The excess thionyl chloride was removed by distillation under reduced pressure.



**Scheme 1.26.** Synthetic scheme of **1.34**.

### Synthesis of 1-(cyclohepta-2,4,6-trien-1-yl)-2-diazoethan-1-one **1.35** and barbaralone **1.11**

There are two synthetic steps remaining in order to synthesise barbaralone. We attempted the first step which is converting the acid chloride **1.34** into the diazoketone **1.35** using diazomethane. The second step uses CuSO<sub>4</sub> to stabilise the carbene and synthesise the final compound **1.11**. Diazomethane which is used in the first step is prepared from *N*-methyl-*N*-nitrosourea and KOH. Considering diazomethane is highly toxic and explosive, the synthetic step is carried carefully in the fumehood. The solution is kept at 0 °C and slowly added into the acid chloride solution, and the bottleneck should only be sealed with cotton to prevent explosion. After the reaction is set up, the flask containing the diazomethane solution was allowed to stand in the fume cupboard until the yellow color completely faded. The crude product was then carried into the final step without further purification, however the <sup>1</sup>H NMR data was not consistent with the barbaralone obtained via Echavarren's gold(I) catalyst method. Initially, we assumed that the CuSO<sub>4</sub> did not work, so we attempted this step again with Rh<sub>2</sub>(CH<sub>3</sub>COO)<sub>4</sub> as the catalyst, but it was not successful either (Scheme 1.27). Upon repeating the diazomethane reaction and checking the crude <sup>1</sup>H NMR, we noticed that every time the NMR peaks were a bit different, since the NMR data of the diazoketone **1.35** was not reported in the original literature, we could not decide whether the diazomethane reaction really worked. It is possible that using diazomethane to get diazoketone **1.35** is not a stable and promising method, therefore there is difficulty executing the experimental and it is hard to control due to its toxicity. Currently, we are looking to find another promising route to achieve **1.35**.



**Scheme 1.27.** Failed attempts to synthesize diazoketone **1.35** and barbaralone **1.11**.

## 1.8 Conclusions and Future Work

The aim of this work has been to integrate and improve the traditional synthetic routes of making barbaralone, attempting to scale up the synthesis so that the cost overall is much cheaper. As an important building block, achieving a more efficient method to synthesis barbaralone **1.11** will allow further synthesis and investigation of derivatives. At this moment in time, three out of the five synthetic steps have been successfully achieved, in which the hydrolysis step of ester **1.32** was improved after the literature conditions failed. Currently the bottleneck is the conversion of acid chloride **1.34** into the diazoketone **1.35**. At this moment in time, this step has not been successful using diazomethane. The existing methods of making diazoketones are all based on similar principles, however some methods utilize trimethylsilyldiazomethane instead of diazomethane. Considering its explosive hazard is relatively low, this reagent will be attempted in the reaction in the near future. After the five steps are all successfully completed, the obtained barbaralone will be used to synthesize various derivatives and we will investigate the effect of noncovalent control over their equilibrium distribution in the solution state, including the capsulation of cyclodextrin as well as coordination with metal ions. However, the traditional routes were reported nearly half a century ago, thus it is possible that some errors are reported due to the limitation of experimental and analysis methods. If these current synthetic routes cannot be optimised, we will follow the gold(I) catalyst route to obtain barbaralone.

## 1.9 Experimental

### 1.9.1 General Methods

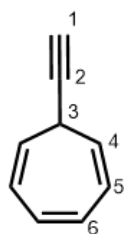
Unless otherwise stated, all reagents were purchased from commercial suppliers (Sigma-Aldrich,

Acros Organics, or Fischer Scientific) and used without further purification. Air-sensitive reactions were carried out under a nitrogen atmosphere using Schlenk techniques. Purification by flash column chromatography was carried out using a Teledyne Isco CombiFlash Rf+ system, with pre-packed SiO<sub>2</sub> columns as the stationary phase. Analytical TLC was performed on neutral aluminium sheet silica gel plates and visualised under UV irradiation (254 nm).

Solution-phase NMR spectra were recorded using a Bruker Advance (III)-400 (<sup>1</sup>H 400.130 MHz and <sup>13</sup>C 100.613 MHz), Varian VNMRS-600 (<sup>1</sup>H 600.130 MHz and <sup>13</sup>C 150.903 MHz) or a Varian V-NMRS-700 (<sup>1</sup>H 700.130 MHz and <sup>13</sup>C 176.048 MHz) spectrometer, at a constant temperature of 298 K unless otherwise stated. Chemical shifts are reported in parts per million (ppm) relative to residual non-deuterated solvents [CDCl<sub>3</sub>; δ = 7.26 or 77.16]. Coupling constants (J) are reported in hertz (Hz). NMR spectra were processed using MestReNova version 12.0.3. Data are reported as follows: chemical shift, multiplicity, coupling constants, integration and assignment. Multiplicities are reported as singlet (s), doublet (d), triplet (t), and multiplet (m).

High-resolution ESI-MS were performed using a Waters TQD UPLC ES MS/MS spectrometer.

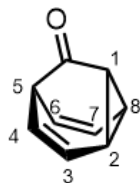
### 1.9.2 Synthetic Procedures



#### 7-Ethynylcyclohepta-1,3,5-triene **1.63**:

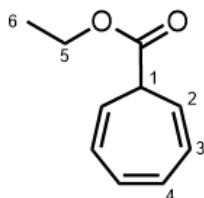
LiCl (0.524 g, 12.4 mmol) was dried overnight under vacuum at 60 °C, then added to anhydrous THF and cooled to -78 °C. Ethynyl magnesium bromide (0.5 M in THF, 22.5 mL, 12.2 mmol) was added and stirred for 10 min at this temperature. Solid tropylium tetrafluoroborate (1.00 g, 5.62 mmol) was added to the reaction mixture and stirred at this temperature for 10 min. The mixture was allowed to warm to rt and left to stir for 16 h. The reaction was quenched with NH<sub>4</sub>Cl solution (50 mL), then extracted with Et<sub>2</sub>O (3 × 50 mL) and brine (20 mL). The organic extracts were dried with MgSO<sub>4</sub> and concentrated under reduced pressure (rotary evaporator bath at 16 °C, ≥ 100 mbar). The crude residue was purified via column chromatography (Teledyne Isco CombiFlash Rf+ system, 24 g SiO<sub>2</sub>, isocratic n-pentane elution) to give 7-ethynylcyclohepta-1,3,5-triene as a yellow oil (0.998 g, yield > 100% due to the existence of solvent). <sup>1</sup>H NMR (600 MHz, CDCl<sub>3</sub>): δ 6.68 (m, 2H, H<sub>6</sub>), 6.21 (m, 2H, H<sub>5</sub>), 5.36 (m,

2H, H<sub>4</sub>), 2.54 (m, 1H, H<sub>3</sub>), 2.19 (d, *J* = 2.6 Hz, 1H, H<sub>1</sub>). Characterization data are consistent with those reported previously: *Organometallics* 2018, **5**, 781–786.



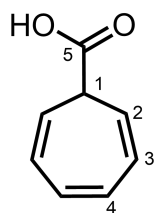
**Tricyclo[3.3.1.0]nona-3,6-dien-9-one (barbaralone 1.11):**

7-Ethynylcyclohepta-1,3,5-triene (596 mg, 5.13 mmol) and diphenyl sulfoxide (2.09 g, 10.3 mmol) were dissolved in anhydrous CH<sub>2</sub>Cl<sub>2</sub> (52 mL). (Acetonitrile)[1,3-bis(2,6-diisopropylphenyl)imidazol-2-ylidene]gold(I) tetrafluoroborate catalyst (0.186 g, 0.250 mmol, 5 mol%) was added to the reaction mixture and stirred overnight. The reaction was quenched with 10 drops of Et<sub>3</sub>N and concentrated under reduced pressure. The crude product was purified *via* column chromatography (Teledyne Isco CombiFlash Rf+ system, 12 g SiO<sub>2</sub>, hexanes-EtOAc, gradient elution) to give the title compound as a yellow-coloured solid (143 mg, 1.08 mmol, 24% yield). <sup>1</sup>H NMR (600 MHz, CDCl<sub>3</sub>): δ 5.77 (m, 2H, H<sub>1/5</sub>), 4.35 (s, 4H, H<sub>2/4/6/8</sub>), 2.77 (t, *J* = 8.7 Hz, 2H, H<sub>3/7</sub>). Characterization data are consistent with those reported previously: *Angew. Chem. Int. Ed.* 2016, **37**, 11178–11182.



**Ethyl cyclohepta-2,4,6-triene-1-carboxylate 1.32:**

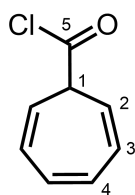
Rh(O<sub>2</sub>CF<sub>3</sub>)<sub>2</sub> (0.132 g, 0.200 mmol) was dissolved in benzene (78.1 g, 89.4 mL). Ethyl diazoacetate (5.15 g, 4.75 mL, 45.1 mmol) was added to the Rh(O<sub>2</sub>CCF<sub>3</sub>)<sub>2</sub> solution with an automatic syringe pump over 2 h. After complete addition of the ethyl diazoacetate, benzene was removed under reduced pressure to give the title compound as brown oil (6.36 g, 38.7 mmol, 86% yield). <sup>1</sup>H NMR (600 MHz, CDCl<sub>3</sub>): δ 6.74 - 6.64 (m, 2H, H<sub>4</sub>), 6.36 - 6.23 (m, 2H, H<sub>3</sub>), 5.52 - 5.43 (m, 2H, H<sub>2</sub>), 4.29 (q, *J* = 7.2 Hz, 2H, H<sub>5</sub>), 2.57 (tt, *J* = 5.6, 1.5 Hz, 1H, H<sub>1</sub>), 1.34 (t, *J* = 7.1, 0.6 Hz, 3H, H<sub>6</sub>). Characterization data are consistent with those reported previously: *Org. Lett.* 2017, **19**, 5268–5271.



**Cyclohepta-2,4,6-triene-1-carboxylic acid 1.33:**

Ethyl cyclohepta-2,4,6-triene-1-carboxylate (5.0 g, 30.5 mmol) was dissolved in mixture of EtOH (20 mL) and THF (60 mL) and was then stirred at 0°C. LiOH (0.877 g, 36.6 mmol) was dissolved in H<sub>2</sub>O (37 mL) and added into the organic

solution. The mixture was stirred at 0 °C for 3 h. The aqueous phase was separated and acidified with HCl until pH=1 was reached. It was extracted with EtOAc (50 mL) and dried with MgSO<sub>4</sub>. The organic solvents was removed under reduced pressure to give the title compound as brown oil (2.73 g, 20.0 mmol, 66% yield). <sup>1</sup>H NMR (600 MHz, CDCl<sub>3</sub>): δ 6.75 - 6.61 (m, 2H, H<sub>4</sub>), 6.32 (m, 2H, H<sub>3</sub>), 5.49 - 5.33 (m, 2H, H<sub>2</sub>), 2.62 (tt, *J* = 5.6, 1.2 Hz, 1H, H<sub>1</sub>). <sup>13</sup>C NMR (151 MHz, CDCl<sub>3</sub>) δ 173.09 (C<sub>5</sub>), 130.78 (C<sub>4</sub>), 125.49 (C<sub>3</sub>), 117.00 (C<sub>2</sub>), 43.04 (C<sub>1</sub>). **HR-ESI MS**: *m/z* = 137.1673 [M+H]<sup>+</sup>, calculated for C<sub>8</sub>H<sub>9</sub>O<sub>2</sub><sup>+</sup>: 137.0602.

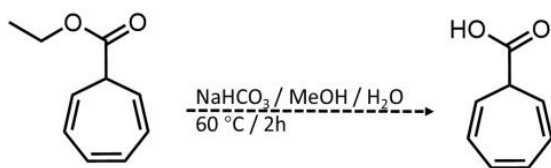


**Cyclohepta-2,4,6-triene-1-carbonyl chloride 1.34:**

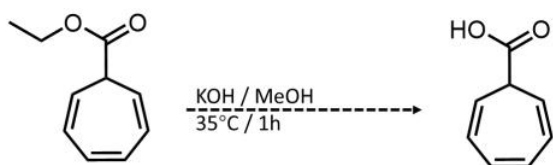
Cyclohepta-2,4,6-triene-1-carboxylic acid (2.73 g, 20.0 mmol) was dissolved in SOCl<sub>2</sub> (22 mL) and stirred at room temperature for 42 h. The SOCl<sub>2</sub> was removed under reduced pressure at 60 °C to give the title compound as a brown oil (2.72 g, 17.6 mmol, 88% yield). <sup>1</sup>H NMR (600 MHz, CDCl<sub>3</sub>): δ 6.67 (m, *J* = 4.1, 2.7, 0.8 Hz, 2H, H<sub>4</sub>), 6.40 (m, *J* = 8.6, 4.1, 2.8, 0.9 Hz, 2H, H<sub>3</sub>), 5.33 (m, *J* = 8.6, 6.0, 0.9 Hz, 2H, H<sub>2</sub>), 3.17 - 2.98 (m, 1H, H<sub>1</sub>). <sup>13</sup>C NMR (151 MHz, CDCl<sub>3</sub>) δ 160.51 (C<sub>5</sub>), 130.19 (C<sub>4</sub>), 125.78 (C<sub>3</sub>), 110.61 (C<sub>2</sub>), 52.38 (C<sub>1</sub>). **HR-ESI MS**: *m/z* = 155.1432 [M+H]<sup>+</sup>, calculated for C<sub>8</sub>H<sub>8</sub>ClO<sup>+</sup>: 155.0263.

**1.9.3 Failed Reactions**

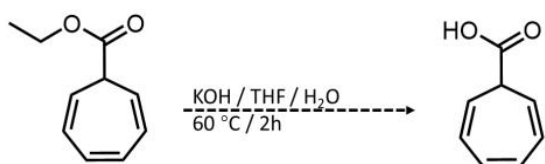
**Cyclohepta-2,4,6-triene-1-carboxylic acid 1.33:**



Ethyl cyclohepta-2,4,6-triene-1-carboxylate (500 mg, 3.05 mmol) was dissolved in MeOH (4 mL). NaHCO<sub>3</sub> (380 mg, 4.52 mmol) was dissolved in H<sub>2</sub>O (3 mL). The aqueous solution was added into the organic solution and refluxed 60 °C for 2 h. The aqueous phase was separated and washed with hexane (2 × 13 mL). It was acidified with H<sub>2</sub>SO<sub>4</sub>, extracted with hexanes (30 mL) and dried with MgSO<sub>4</sub>. The hexane was removed under reduced pressure to give the title compound as a brown oil. Characterization data are not consistent with those reported previously: *J. Org. Chem.* 1987, **52**, 2666–2673.



Ethyl cyclohepta-2,4,6-triene-1-carboxylate (50.0 mg, 0.310 mmol) was dissolved in MeOH (3 mL) and stirred at 35 °C. KOH (67.0 mg, 1.19 mmol) was added into the solution and stirred for 1 h. The aqueous phase was separated, acidified with H<sub>2</sub>SO<sub>4</sub> until pH=1 was reached, extracted with hexane (10 mL) and dried with MgSO<sub>4</sub>. The hexanes were removed under reduced pressure to give the product as a brown oil. Characterization data are not consistent with those reported previously: *J. Org. Chem.* 1987, **52**, 2666–2673.



Ethyl cyclohepta-2,4,6-triene-1-carboxylate (100 mg, 0.664 mmol) was dissolved in THF (14 mL). KOH (10.9 g, 194 mmol) was dissolved in H<sub>2</sub>O (13 mL). The aqueous solution was added into the organic solution and refluxed at 60 °C for 2 h. The aqueous phase was separated, acidified with HCl until pH=1 was reached, extracted with EtOAc and dried with MgSO<sub>4</sub>. The ethyl acetate was removed under reduced pressure to give the product as a brown oil. Characterization data are not consistent with those reported previously: *J. Org. Chem.* 1987, **52**, 2666–2673.



Ethyl cyclohepta-2,4,6-triene-1-carboxylate (100 mg, 0.664 mmol) was dissolved in THF (10 mL). Acid (1 N, 10 mL) was added and stirred under gradient temperature. Upon completion of the reaction which is monitored via TLC, the <sup>1</sup>H-NMR data of reaction mixture was obtained and compared to the literature data.

Different acids were used over three trails:

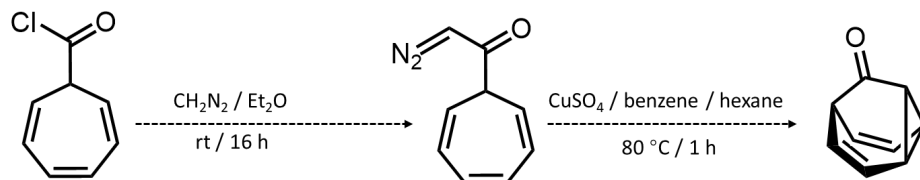
Trail 1: HCl, the TLC stain disappeared at 50 °C

Trail 2: H<sub>2</sub>SO<sub>4</sub>, the TLC stain disappeared at 35 °C

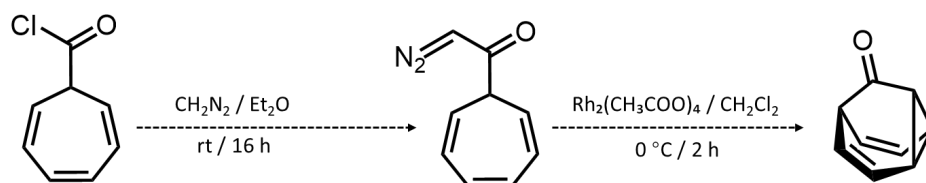
Trail 3: AcOH, the TLC stain disappeared at 35 °C

Characterization data of all trails are not consistent with those reported previously: *J. Org. Chem.* 1987, **52**, 2666–2673.

**1-(cyclohepta-2,4,6-trien-1-yl)-2-diazoethan-1-one 1.35 and barbaralone 1.11:**



KOH (2.00 g, 51.2 mmol) was dissolved in  $\text{H}_2\text{O}$  (20 mL). The solution was combined with diethyl ether (4 mL) and cooled to  $0\text{ }^\circ\text{C}$  in a Conical flask. *N*-methyl-*N*-nitrosourea (500 mg, 4.85 mmol) was added into the combined solution. The flask was allowed to stand in the fumehood with the bottleneck sealed with cotton until all solid was dissolved to obtain the  $\text{Et}_2\text{O}$  solution of diazomethane. The solution was slowly poured into another Conical flask containing KOH pellets at  $0\text{ }^\circ\text{C}$  and allowed to stand for 5 min with the bottleneck sealed with cotton. Cyclohepta-2,4,6-triene-1-carbonyl chloride (500 mg, 3.23 mmol) was dissolved in  $\text{Et}_2\text{O}$  (20 mL). The prepared diazomethane solution was slowly poured into the acid chloride solution and allowed to stand in the fumehood with the bottleneck sealed with cotton for 16 h at room temperature. The reaction solution was filtered and concentrated under reduced pressure. No further purification was required.  $\text{CuSO}_4$  (300 mg, 4.72 mmol) was dried for 2 h under vacuum at  $200\text{ }^\circ\text{C}$ , added into hexane (3 mL) and kept refluxing at  $80\text{ }^\circ\text{C}$  under  $\text{N}_2$ . The crude product of **1.35** was dissolved in benzene (2 mL) and hexane (2 mL). The solution was added dropwise into the  $\text{CuSO}_4$  suspension over 45 min. The reaction mixture was kept refluxing under  $\text{N}_2$  for 1 h. The solution was filtered and concentrated under reduced pressure. Characterization data are not consistent with the barbaralone obtained using the gold(I) catalyst procedure.



KOH (2.00 g, 51.2 mmol) was dissolved in  $\text{H}_2\text{O}$  (20 mL). The solution was combined with  $\text{Et}_2\text{O}$  (4 mL) and cooled to  $0\text{ }^\circ\text{C}$  in a Conical flask. *N*-methyl-*N*-nitrosourea (500 mg, 4.85 mmol) was added into the combined solution. The flask was allowed to stand in the fume cupboard with the

bottleneck sealed with cotton until all solid was dissolved to obtain the Et<sub>2</sub>O solution of diazomethane. The solution was slowly poured into another Conical flask containing KOH pellets at 0 °C and allowed to stand for 5 min with the bottleneck sealed with cotton. Cyclohepta-2,4,6-triene-1-carbonyl chloride (500 mg, 3.23 mmol) was dissolved in Et<sub>2</sub>O (20 mL). The prepared diazomethane solution was slowly poured into the acid chloride solution and allowed to stand in the fumehood with the bottleneck sealed with cotton for 16 h at room temperature. The reaction solution was filtered and concentrated under reduced pressure. No further purification was required. Rh<sub>2</sub>(CH<sub>3</sub>COO)<sub>4</sub> (29 mg, 0.07 mmol) was dissolved in CH<sub>2</sub>Cl<sub>2</sub> (5 mL) and kept at 0 °C. The crude product of diazoketone was dissolved in CH<sub>2</sub>Cl<sub>2</sub> (5 mL), one half of the Rh<sub>2</sub>(CH<sub>3</sub>COO)<sub>4</sub> solution was added dropwise over 20 min and the reaction mixture was stirred for 1 h at room temperature. The mixture was cooled to 0 °C, the remaining half of diazoketone solution was added dropwise over 20 min and the reaction mixture was stirred for another 1 h at rt. The reaction solution was filtered and concentrated under reduced pressure. Characterization data are not consistent with the barbaralone obtained using the gold(I) catalyst procedure.

## 1.10 Appendices

No additional information was required. All mass spectrometry data, NMR spectra and other analytical data can be found on the McGonigal group shared folder.

(\\prsbblue02.mds.ad.dur.ac.uk\vnvr72\PM\Yuzhen Wen)

## 1.11 References

1. (a) W. von E. Doering and W. R. Roth, *Tetrahedron*. 1963, **19**, 175; (b) G. Schröder, *Angew. Chem.* 1963, **75**, 722; *Angew. Chem. Int. Ed. Engl.* 1963, **2**, 481; (c) A. Adult, *J. Chem. Educ.* 2001, **78**, 924; (d) H. G. Viehe, *Angew. Chem. Int. Ed. Engl.* 1965, **4**, 746.
2. (a) P. Ahlberg, D. L. Harris and S. Winstein, *J. Am. Chem. Soc.* 1970, **92**, 5545; (b) D. Cremer, P. Svensson, E. Kraka and P. Ahlberg, *J. Am. Chem. Soc.* 1993, **115**, 7445; (c) P. Ahlberg, J. B. Grutzner, D. L. Harris and S. Winstein, *J. Am. Chem. Soc.* 1970, **92**, 3478; (d) B. Grutzner and S. Winstein, *J. Am. Chem. Soc.* 1970, **92**, 3186; (e) P. Ahlberg, D. L. Harris and S. Winstein, *J. Am. Chem. Soc.* 1970, **92**, 2146.
3. (a) J. G. Henkel and J. T. Hane, *J. Org. Chem.* 1983, **48**, 3858; (b) C. Engdahl and P. Ahlberg, *J. Am. Chem. Soc.* 1979, **101**, 3940; (c) L. G. Greifenstein, J. B. Lambert, M. J. Broadhurst, L. A. Paquette, *J. Org. Chem.* 1973, **38**, 1210; (d) G. G. Cristoph, S. Hardwick, U. Jacobsson Y.-B. Koh, R. Moerck and L. A. Paquette, *Tetrahedron. Lett.* 1977, **14**, 1249.
4. H. E. Zimmerman and G. L. Grunwald, *J. Am. Chem. Soc.* 1996, **88**, 183.
5. (a) A. R. Lippert, V. L. Keleshian and J. W. Bode, *Org. Biomol. Chem.* 2009, **7**, 1529; (b) K. K. Larson, M. He, J. F. Teichert, A. Naganawa and J. W. Bode, *Chem. Sci.* 2012, **3**, 1825.
6. A. N. Bismillah, J. Sturala, B. M. Chapin, D. S. Yufit, P. Hodgkinson and P. R. McGonigal, *Chem. Sci.* 2018, **9**, 8631–8636.
7. A. C. Cope and E. M. Hardy, *J. Am. Chem. Soc.* 1940, **62**, 441.
8. M. B. Smith and J. March, *March's Advanced Organic Chemistry*, 2007, 1659–1673.
9. (a) W. von E. Doering and J. W. Rosenthal, *J. Am. Chem. Soc.* 1966, **88**, 2078; (b) M. Jones and L. T. Scott, *J. Am. Chem. Soc.* 1967, **89**, 150.
10. S. Ferrer and A. M. Echavarren, *Synthesis*. 2019, **51**, 1037.
11. J. Font, F. López and F. Serratosa, *Tetrahedron. Lett.* 1972, **13**, 2589.
12. W. von E. Doering, B. M. Ferrer, E. T. Fossel, J. H. Hatenstein, M. Jr. Jones, G. Klumpp, R. M. Rubin and M. Saunders, *Tetrahedron*. 1967, **23**, 3943.
13. J. F. M. Oth, R. Merényi, J. Nielsen and G. Schröder, *Chem. Ber.* 1965, **98**, 3358.
14. (a) G. Schröder and J. F. M. Oth, *Angew. Chem. Int. Ed. Engl.* 1967, **6**, 414; (b) J. F. M. Oth, R. Merényi, G. Engel and G. Schröder, *Tetrahedron. Lett.* 1966, **7**, 3377.
15. A. R. Lippert, J. Kawobamrung and J. W. Bode, *J. Am. Chem. Soc.* 2006, **128**, 14738.
16. T. Mukaiyama, *Angew. Chem. Int. Ed. Engl.* 1977, **16**, 817.

17. A. E. Greene and M. T. Edgar, *J. Org. Chem.* 1989, **54**, 1468.
18. O. Yahiaoui, L. F. Pašteka, B. Judeel and T. Fallon, *Angew. Chem. Int. Ed.* **2018**, *57*, 2570.
19. O. Yahiaoui, L. F. Pašteka, C. J. Blake, C. G. Newton and T. Fallon, *Org. Lett.* 2019, **21**, 9574–9578
20. (a) A. R. Lippert, A. Naganawa, V. L. Keleshian and J. W. Bode, *J. Am. Chem. Soc.* 2010, **132**, 15790; (b) M. He, J. W. Bode, *Proc. Natl. Acad. Sci. USA.* 2011, **108**, 14752; (c) M. He, J. W. Bode, *Org. Biomol. Chem.* 2013, **11**, 1306.
21. W. von E. Doering and W. R. Roth, *Angew. Chem. Int. Ed. Engl.* 1963, **2**, 115.
22. (a) L. A. Paquette, U. Jacobsson and M. Oku, *J. C. S. Chem. Comm.* 1975, 115; (b) L. G. Griefenstein, J. B. Lambert, M. J. Broadhurst and L. A. Paquette, *J. Org. Chem.* 1973, **38**, 1211.
23. R. H. Shapiro, *Org. React.* 1976, **23**, 405.
24. H. Quast, M. Witzel, E. –M. Peters, K. Peters and H. G. von Schnering, *Leibigs. Ann.* 1995, 725.
25. (a) H. Kessler and W. Ott, *J. Am. Chem. Soc.* 1976, **98**, 5014; (b) A. McKillop and J. A. Tarbin, *Tetrahedron. Lett.* 1983, **24**, 1505.
26. H. Quast, C. Becker, M. Witzel, E. –M. Peters, K. Peters and H. G. von Schnering, *Leibigs. Ann.* 1996, 985.
27. (a) P. R. McGonigal, C. de León, Y. H. Wang, A. Homs, C. R. Solorio-Alvarado and A. M. Echavarren, *Angew. Chem. Int. Ed.* 2012, **51**, 13093; (b) S. Ferrer and A. M. Echavarren, *Angew. Chem. Int. Ed.* 2016, **55**, 11178.
28. A. N. Bismillah; B. M. Chapin; B. A. Hussein and P. R. McGonigal. *Chem. Sci.* 2020, **11**, 324–332.
29. (a) G. Schröder and W. Witt, *Angew. Chem. Int. Ed.* 1979, **18**, 311; (b) K. Sarama, W. Witt and G. Schröder, *Chem. Ber.* 1983, **116**, 3800.
30. J. F. Teichert, D. Mazunin and J. W. Bode, *J. Am. Chem. Soc.* 2013, *135*, 11314.7.
31. A. J. Anciaux, A. Demonceau, A. F. Noels, A. J. Hubert, R. Warin, and P. Teyssié, *J. Org. Chem.* 1981, **46**, 873–876.
32. A. Facchetti and A. Streitwieser, *J. Org. Chem.* 1999, **64**, 2281–2286.
33. A. N. Bismillah, PhD Thesis, Durham University, 2019.

## Chapter 2

### 2.1 Chirality

The term chirality originates from the Greek word “hkeir”, which means hand and describes objects that exist as a pair of mirror images, which are called enantiomers. Chirality in molecules was firstly discovered by Pasteur in 1848 when he was studying tartaric acid and racemic acid.<sup>1</sup> It has been a fundamental concept in chemistry research and has been widely applied in various fields.

Molecules and molecular systems can achieve chirality by arranging atoms asymmetrically in the space around the center, axis, or plane, called points, axes, and plane chirality, respectively. Not only covalently bonded molecules with a defined structure, but also noncovalently interacting supramolecular assemblies with conformational flexibilities can form chiral structures.<sup>2</sup>

In supramolecular chemistry, the conformational chirality results from rearrangement or assembly under a chiral influence that removes the symmetry elements from a molecule. It can occur through the supramolecular interactions with chiral inducers, or through an intramolecular chiral conformation which is maintained by the steric hindrance to prevent the racemization.

#### 2.1.1 Dynamic Chirality

Dynamic chirality is a phenomenon which occurs through the low-energy barrier of racemization, allowing the mutual conversion of enantiomers. The pyramidal inversion of nitrogen and phosphorous species has led to their domination of dynamic chirality at the stereogenic center. The energy barrier of the inversion of nitrogen atoms is relatively low, thus the isomers could be inverted at room temperature and are difficult to be separated. While for phosphorous atoms, the energy barrier is higher, and the isomers could exist stably.

For carbon atoms, generally the stereogenic center is stable without breaking bonds, there are still examples of their enantiomerization.<sup>3</sup> The latest example was reported by Miller and co-workers in 2017, in which the dynamic chirality was exhibited through redox interconversion.<sup>4</sup> (Figure 2.1)<sup>36</sup> The main limitation of redox interconversion is that it remains in the solid state and cannot be switched off, and the redox-active groups must be present in the structure.

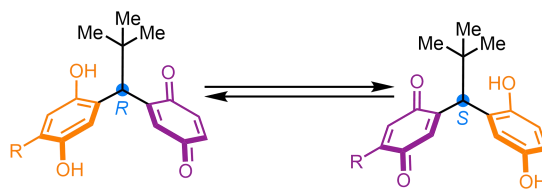


**Figure 2.1** Stereodynamic behaviour through redox interconversion reported by Miller and coworkers.

The rapid and reversible Cope rearrangements occurring in the bullvalene molecule allows a large number of unique shapes to exist in equilibria. Bode has developed the tetra-substituted bullvalenes as adaptive sensors whose equilibrium distribution could be altered by adding analyte and tracked by  $^{13}\text{C}$ -NMR, but the large number of constitutional isomers hindered the specificity of molecules.<sup>5</sup> (Figure 2.2)<sup>36</sup>

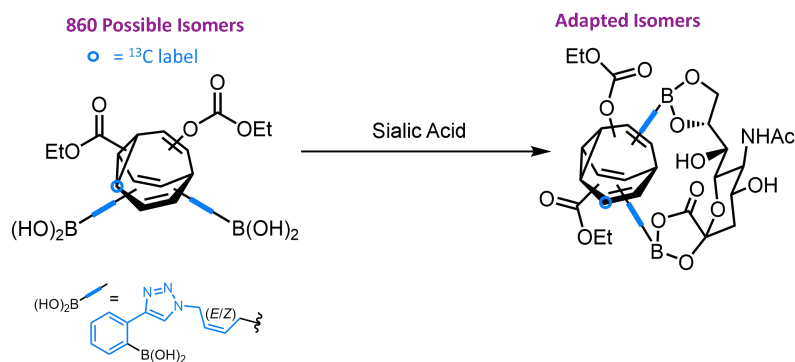


**Figure 2.2.** The tetra-substituted bullvalene showing a shift in equilibrium distribution via sialic acid.

In contrast, barbaralane only has two isomers under Cope rearrangements, thus it is relatively easier to shift the equilibrium distribution of its two isomers in favour of one the in solution and solid state, and analyse this behaviour detailedly.<sup>6</sup> The barbaralane derivatives that equilibrate between two isomers in solution could be resolved to a single isomer in the solid state, which could be achieved via both covalent (addition of a chiral tether) and noncovalent control (molecular recognition of macrocyclic hosts such as  $\beta$ -cyclodextrin). (Figure 2.3)<sup>36</sup>

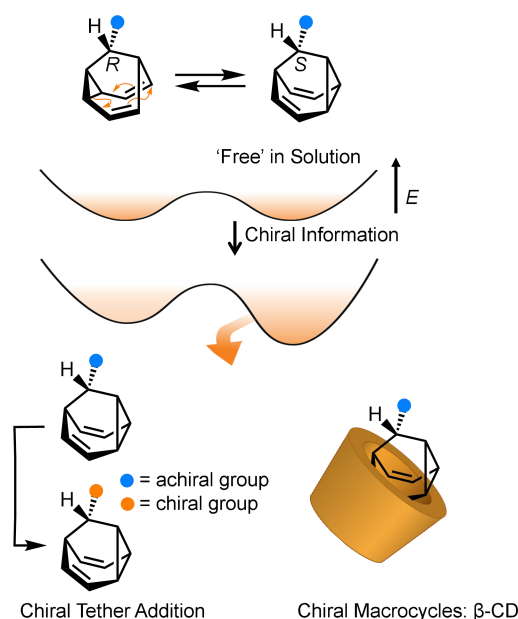


**Figure 2.3.** The effect of covalent and noncovalent control on relative energies of stereochemistry of barbaralanes.

The effects of crystallization on barbaralane isomerization equilibria have been reported by McGonigal in 2018.<sup>7</sup> Five different barbaralane derivatives were investigated, and three of them were observed to have the same constitution as their major solution-phase isomer while the other two had the minor solution-phase isomer. The results demonstrated that their crystallization is directed by the molecular size and shape of the isomers.

### 2.1.2 Noncovalent Control

The noncovalent control of chirality generally includes hydrogen bonding,  $\pi$ -stacking, coordination, and electrostatic interactions.<sup>8</sup>

The pool of chiral building blocks based on hydrogen bonding is large and diverse. Many building blocks are easily available from natural sources such as carbohydrates and amino acids. One of the earliest examples of hydrogen bonding system was reported by Reinhoudt in 1997, in which they added barbituric or cyanuric acid to the dimelamine calix[4]arenes **2.2** to form nine-component [3+6] rosettes by 36 hydrogen bonds and stacking interactions of  $\pi$ -surfaces.<sup>9</sup> (Figure 2.4) The rosettes exhibits supramolecular chirality due to the D<sub>3</sub>-symmetric arrangement of melamine fragments, and they are stable enough to be isolated as single enantiomers with either *P*(all-*S*) or *M*(all-*R*) helicity. When the enantiomerically pure chiral dimelamine **2.1** was added, only a single

diastereoisomeric rosette was formed. Reinhoudt also demonstrated that the chirality of the rosettes is dynamic and can undergo exchange under similar conditions.<sup>10</sup>

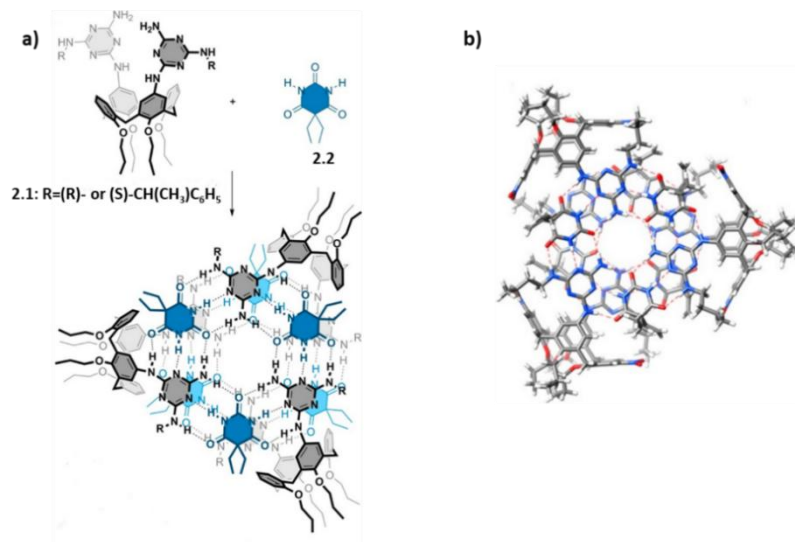


**Figure 2.4.** (a) The self-assembly of dimelamine calix[4]arene **2.1** and diethylbarbituric acid **2.2**. (b) X-ray structure of rosette built from achiral **2.2** and calix[4]arene dimelamine when R = C<sub>4</sub>H<sub>9</sub>.<sup>9</sup>

Hydrogen bonding is also possible to form between two properly oriented carboxylic acids or between a carboxylic acid and an amidine. In 2015, Yashima reported artificial chirality-selective chiral dimer chains bearing carboxylic acid or amidine groups joined by chiral amide linkers with different sequences.<sup>11</sup> In chloroform, the dicarboxylic acid **2.3a** self-assembles into tightly folded dimers with a ratio of 2:1 between the homochiral and heterochiral dimer. **2.3b** self-sorts in a completely homochiral way, and forms ion pairs with diamidine **2.4a**. For more flexible ligands such as ureidopyrimidinones **2.5** and **2.6**, helical folding and formation of dimers through hydrogen bonding has also been observed. (Figure 2.5)

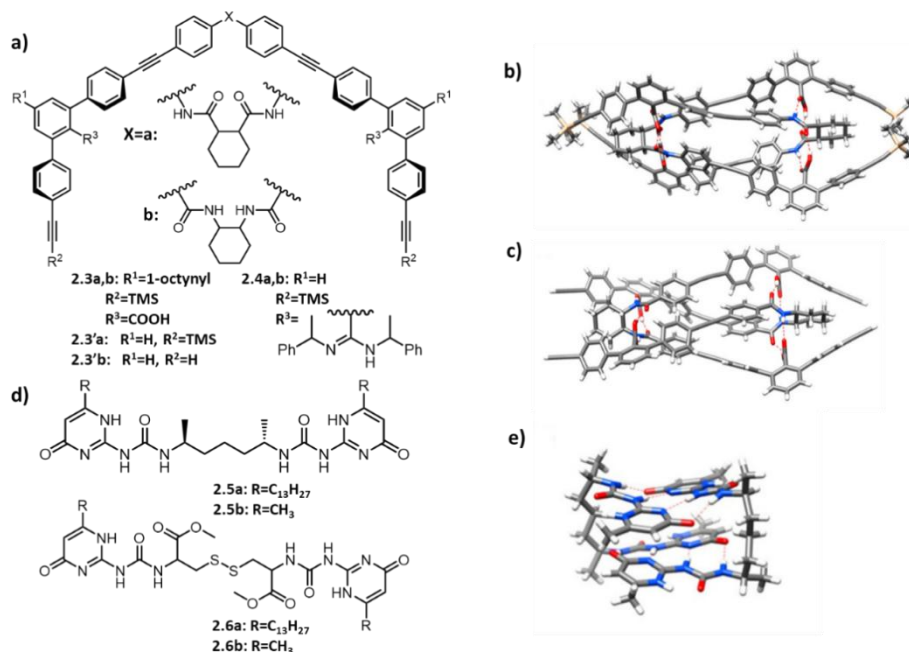


**Figure 2.5.** (a) Structures of carboxylic acids **2.3** and amidines **2.4**. X-ray structures of (b) **2.3'a** and (c) **2.3'b**. (d) Structures of ureidopyrimidinones. (e) X-ray structure of  $((S,S)\text{-}2.6b)_2$ .<sup>11</sup>

Peptides are another type of ideal building block containing a hydrogen bonding system. They have various inherent advantages such as chirality, easy availability, and have a natural tendency to self-assembly. In nature, peptides have two forms of basic secondary structures:  $\alpha$ -helices and  $\beta$ -sheets. (Figure 2.6) The  $\alpha$ -helices are internally self-complementary and unable to be used in artificial systems, while the  $\beta$ -sheets, which includes parallel and antiparallel sheets have been used to induce or direct self-assembly in artificial systems, whereby the chirality control is determined by the interplay between peptide conformational preferences.<sup>8</sup>

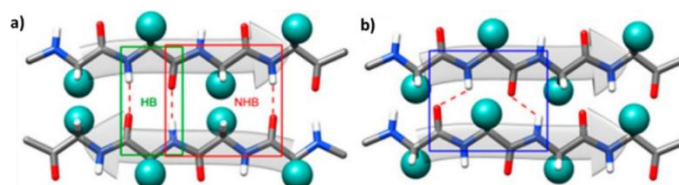


**Figure 2.6.** The two forms of secondary structures of peptides in nature: (a)  $\alpha$ -helices and (b)  $\beta$ -sheets.

The  $\pi$ - $\pi$  stacking usually occurs between molecules with large aromatic faces. One significant advantage is that it can lead to a very tight packing of planar and rigid molecules, which improves the prediction of molecular shapes using geometric features and highly efficient chiral self-sorting.

One example of  $\pi$ - $\pi$  stacking is the dimerization of substituted perylene bisimides (PBIs) through twisted surfaces reported by Wuerthner in 2010: Under the Cotton effect originated from chiral exciton coupling, the dimer of **2.7** was formed through the interaction of unshielded  $\pi$ -surfaces, with a 93% proportion of homochiral dimers.<sup>13</sup> (Figure 2.7)

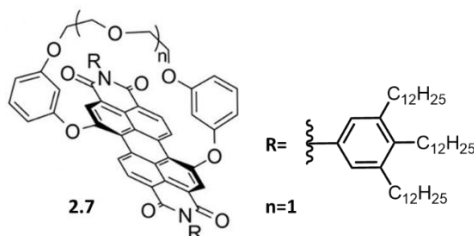


**Figure 2.7.** The structure of substituted perylene bisimide **2.7**.

Electrostatic interactions are considered to be the strongest noncovalent interactions, but their applications are limited by the nondirectional property of electrostatic forces. One of the examples was reported by Ochando in 2006, in which the electrostatic interactions of chiral ammonium picrates **2.8** led to their self-assembly.<sup>14</sup> (Figure 2.8)

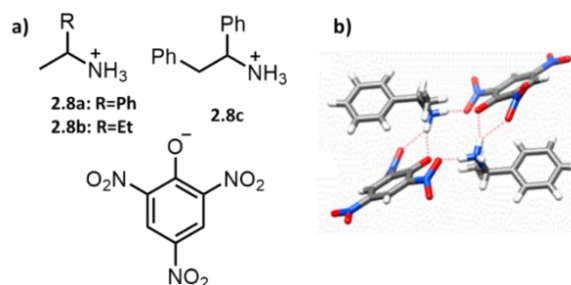


**Figure 2.8.** (a) Chemical structures of ammonium picrates **2.8**. (b) X-ray structure of  $(\mathbf{2.8a})_2$

The most widely used noncovalent interaction to construct chiral structures is coordination bonding. Compared to other interactions, one of its significant advantages is the directionality, which leads to a precise spatial arrangement of ligands. Coordination bonding includes the interactions of metal centers, macrocycles, and cages.

The metal center coordination includes the effect of transition metals, lanthanide metals, and alkali metals. One of the cases of transition metal coordination is the bisoxazoline **2.9** complexes formed with tetrahedral  $\text{Zn}^{2+}$  ions reported by Clark in 2005,<sup>15</sup> in which the enantiomerically pure compound  $(R,R)$ -**2.9** gives homochiral complex with Zn, while the racemic ligand  $\text{rac-2.9}$  gives exclusively to heterochiral complex. (Figure 2.9)

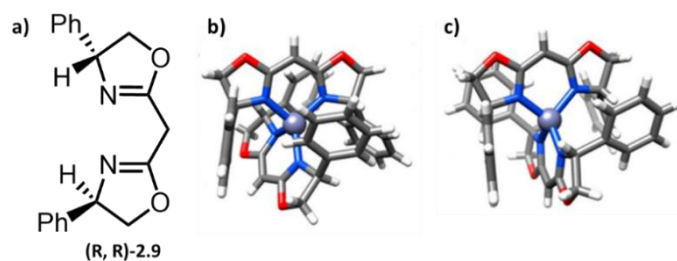


**Figure 2.9.** (a) Chemical structure of bisoxazoline (*R,R*)-**2.9**. X-ray structures of (b) homodimer  $\text{Zn}[(R,R)\text{-2.9}]_2$  and (c) heterodimer  $\text{Zn}[(R,R)\text{-2.9}][(\text{S,S})\text{-2.9}]$ .

Lanthanide metals are big atoms with coordination numbers of seven to ten, which can be affected by the environment and relatively more difficult to be predicted. In 2008, Wilson reported tris(bidentate) complexes formed with chiral ligand **2.10** and  $\text{Y}^{3+}$ ,  $\text{Eu}^{3+}$ , or  $\text{Er}^{3+}$  ions in the THF solution. (Figure 2.10) For the racemic compound, the homochiral  $C_3$ -symmetric complexes are formed preferentially.<sup>16</sup>

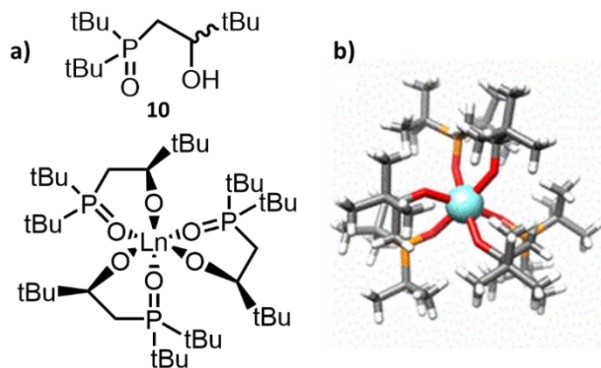


**Figure 2.10.** (a) Chemical structure of alcohol **2.10** and its Ln complexes. (b) X-ray structure of  $\text{Y}(\text{R}\text{-2.10})_3$ .

The interactions of metal coordination can also engage with hydrogen bonding or  $\pi$ - $\pi$  stacking. In 2015, Yashima reported the formation of four-component helicates based on ligand **2.11** and **2.12** or dimers of clothespin-shaped complex **2.14**.<sup>17</sup> In the helicates, the achiral phosphine ligands can exchange with chiral diphosphines **2.13**, in this process, the diphosphines can self-sort in a homochiral way and only complexes with two diphosphines of the same chirality are formed. (Figure 2.11)

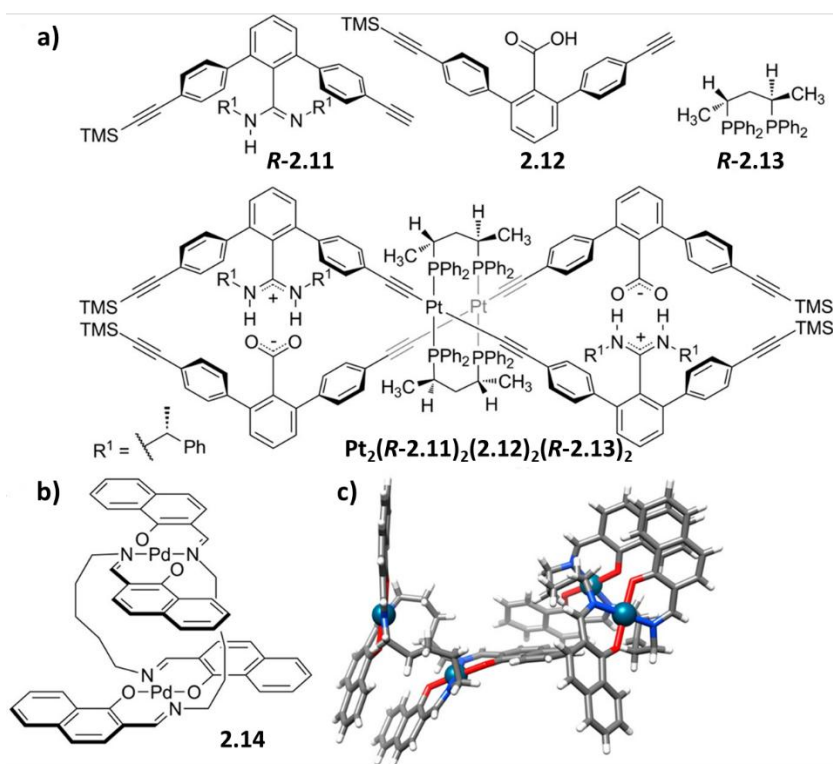


**Figure 2.11.** (a) Structure of *R*-2.11, 2.12, *R*-2.13, and  $\text{Pt}_2(\text{R-2.11})_2(\text{2.12})_2(\text{R-2.13})_2$ . (b) Structure of *anti*-2.14. (c) X-ray structure of the [(+)-2.14][(-)-2.14] dimer.

Macrocycles and cages can also exhibit coordination bonding together with metal ions. The representative molecules are porphyrins, calixsalenes, bipyridines, subphthalocyanines, etc.<sup>8</sup> One of the examples was reported by Osuka in 2008: In porphyrins, the side groups introduce chirality and contain additional coordinating atoms, while in a noncoordinating solvent, the racemic compound **2.15a** and **2.15b** forms a heterochiral dimer through coordination of azanorbornene nitrogen to  $\text{Zn}^{2+}$ .<sup>18</sup> (Figure 2.12)

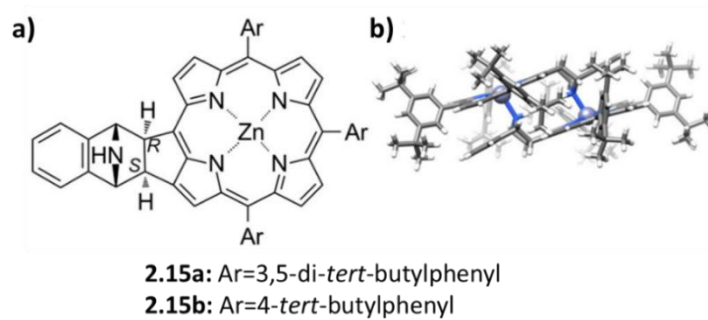


**Figure 2.12.** (a) Chemical structures of **2.15**. (b) X-ray structure of heterochiral dimer  $\text{Zn}_2(\text{2.15a})_2$

## 2.2 Cyclodextrin

Cyclodextrins are a family of cyclic oligosaccharides consisting of a macrocyclic ring of six to eight glucose subunits linked by 1,4-glycosidic bonds. (Figure 2.13) They were firstly discovered by Villers when he degraded the starch with enzymes in 1891.<sup>19</sup> In 1904, Schardinger identified the cyclodextrins as  $\alpha$ -,  $\beta$ -, and  $\gamma$ - according to the number of glucose monomers.<sup>20</sup>

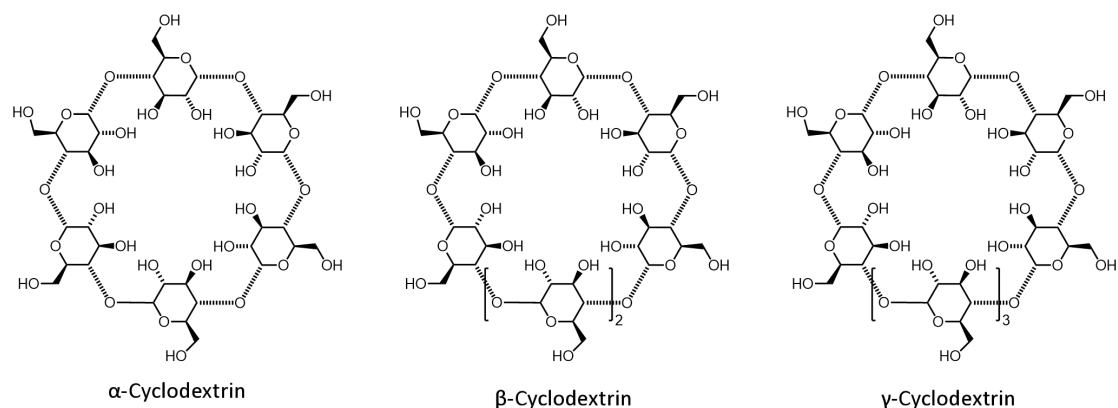


**Figure 2.13.** Chemical structures of  $\alpha$ -,  $\beta$ -, and  $\gamma$ -cyclodextrins.

The D-glucopyranose units in the cyclodextrin molecule are all in chair configuration and cannot rotate freely around the glycosidic bond, giving a conical three-dimensional structure with the secondary hydroxyl groups distributed on the larger opening end and the primary hydroxyl groups on the smaller end. (Figure 2.14) When water is the solvent, the hydroxyl groups can form hydrogen bonds with water molecules, thus allowing the cyclodextrin water-soluble. Another significant feature of the cyclodextrin structure is that it has a hydrophobic cavity. Thus, by utilizing its hydrophobic effect and the volume matching between the host and guest molecules, it can be combined with hydrophobic molecules of suitable size and shape through noncovalent interactions to form stable inclusion compounds. In these inclusion complexes, the guest molecule approaches and penetrates the CD cavity from the more open and accessible secondary hydroxyl side. It is generally recognized that the inclusion phenomena involve weak interactions, such as hydrogen bonds, electrostatic interactions, and van der Waals forces.<sup>21</sup>

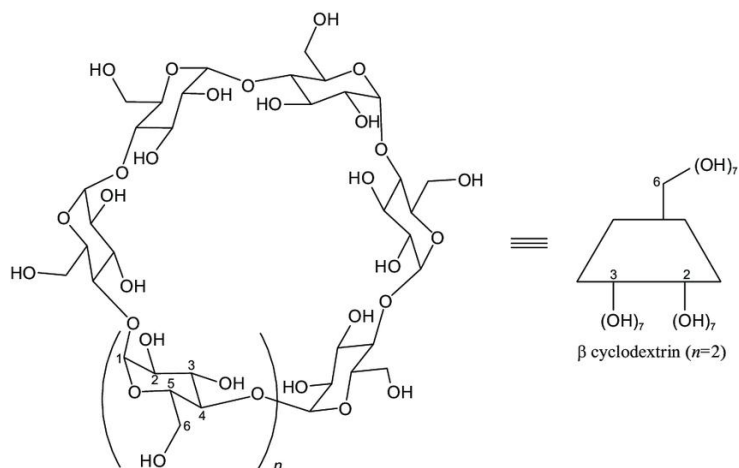


**Figure 2.14.** The configuration and shape of  $\beta$ -cyclodextrin.

The formation of the inclusion complex is usually associated with a favorable enthalpy change and an unfavorable entropy change. Several proposals have been made to explain the favorable enthalpy change such as van der Waals interactions between the guest and the host; hydrogen bonding between the guest and the hydroxyl groups of cyclodextrin; release of high energy water molecules during complex formation as well as the release of strain energy in the macromolecular ring of the cyclodextrin.<sup>23</sup>

The formation of inclusion complexes with guest molecules is one of the most important properties of cyclodextrins. Guest compounds can vary from polar reagents such as acids, amines, small ions, and halogen anions, to highly nonpolar aliphatic and aromatic hydrocarbons. Generally, water is used as the solvent, although there are examples where dimethyl sulfoxide and dimethyl formamide are utilized. The formation of an inclusion complex can alter some of the physical and chemical properties of the guest molecule, such as chemical reactivity, the pK value, solubility as well as various spectral parameters. Thus, the complex formation can be detected by a variety of spectroscopic methods, such as NMR and fluorescence spectroscopies. In 1932, Pringsheim first reported the cyclic oligosaccharide as a host molecule to recognize guest molecules.<sup>24</sup> Then Freudenberg and Cramer synthesized a series of inclusion complexes of cyclodextrins which contained different organic guest molecules. They then investigated their host-guest interactions in water and revealed that no matter how the initial molar ratio of the host and the guest changes, the inclusion complex always has a definite composition in both the solution and the solid states. In

the solution state, the ratio of host to the guest is 1:1, therefore the inclusion complexes are dissolved, an equilibrium is established between dissociated and associated species, which could be expressed by the complex stability constant  $K_a$ .<sup>25</sup>

Cyclodextrin is an ideal host molecule that has been found so far similar to an enzyme and has been widely used in the fields of catalysis, separation<sup>22</sup>, food, and medicine. Amongst the three kinds,  $\beta$ -cyclodextrin is ideal for complexation due to its perfect cavity size, efficient drug complexation and loading, availability, and relatively low cost.

### 2.2.1 Stereoselectivity of Cyclodextrins

Since the cavity of cyclodextrin is restricted in space, it is able to favorably include one conformational isomer of the substrate as a guest than the other and form diastereoisomers. The stereoselectivity of cyclodextrins depends on their size and shape. For  $\beta$ -cyclodextrins, they are often observed as a head-to-head dimer in the crystalline, in which the secondary hydroxyl sides are facing each other and linked with hydrogen bonds, giving a twice cavity volume of the monomer which can encapsulate larger guest molecules.<sup>27</sup>

In 1984, Hirayama included a series of chiral compounds in cyclodextrins and permethylated cyclodextrins, and investigated their chiral recognition through the X-ray data of crystalline complexes.<sup>26</sup> For racemic flurbiprofen, the hydrogen-bonding contact with the carboxyl group of the *R*- and *S*-isomer is different, which was discriminated by the  $\beta$ -cyclodextrin and included respectively, and the *R*-isomer is more favored. For mandelic acid, the inclusion of the *D*-isomer within the permethylated  $\beta$ -cyclodextrin is more favored, for the complex formation with *D*-mandelic acid induces the conformational change of the host molecule so as to include the guest molecule more suitably within the cavity. And the permethylated  $\beta$ -cyclodextrin was proved to be more flexible in the conformational change. This property has been used to isolate racemic compounds and applied in chromatography such as HPLC and capillary electrophoresis.<sup>28</sup>

Cyclodextrins have also been widely used to catalyze chemical reactions such as hydrolysis, oxidation, and substitution.<sup>29</sup> In this process, stereoselective acceleration has been observed and applied. When the included conformational isomer is more reactive than the other one, cyclodextrins exhibit an acceleration effect and vice versa. In the 1970s, Bender has reported both

the stereoselective acceleration and deceleration of cyclodextrins: In the decarboxylation of  $\beta$ -keto acid **2.16**, the preferential inclusion of the more reactive cyclic ground state isomer **2.16b** by cyclodextrins led to a significant acceleration, however, in the reactions of intramolecular carboxylate ion attack in 3-isopropyl glutarate esters **2.17**, one of the conformational isomers was too bulky to fit in the cyclodextrin cavity, which reduced the ground state energy of the esters and led to the deceleration.<sup>30,31</sup>

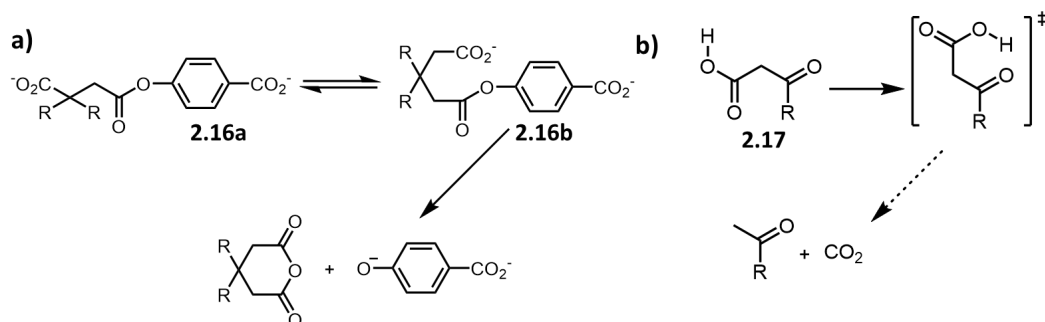


**Figure 2.15.** (a) The acceleration of decarboxylation of  $\beta$ -keto acid. (b) The deceleration of intramolecular carboxylate ion attack of 3-isopropyl glutarate ester.

In recent years, the stereoselectivity of  $\beta$ -cyclodextrin has been utilized in photoreactions.<sup>32</sup> One of the latest examples was reported by Yang and co-workers in 2019, in which they used a series of sulfur- and arene-linked  $\beta$ -cyclodextrin dimers to precisely manipulate the regio- and enantioselectivities of the photocyclodimerization of 2-anthracenecarboxylate to four stereoisomeric classical cyclodimers and two nonclassical cyclodimers, and the *exo*-3-thia- $\beta$ -CD dimer was proved to have much higher selectivities than native  $\beta$ -CD and other  $\beta$ -CD dimers.<sup>33</sup> (Figure 2.16)

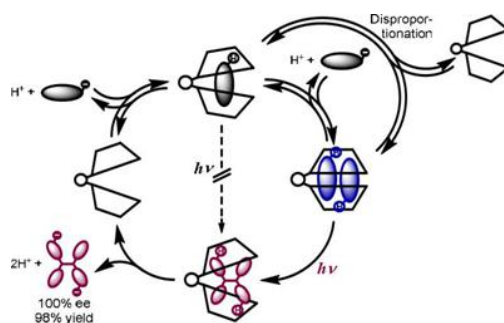
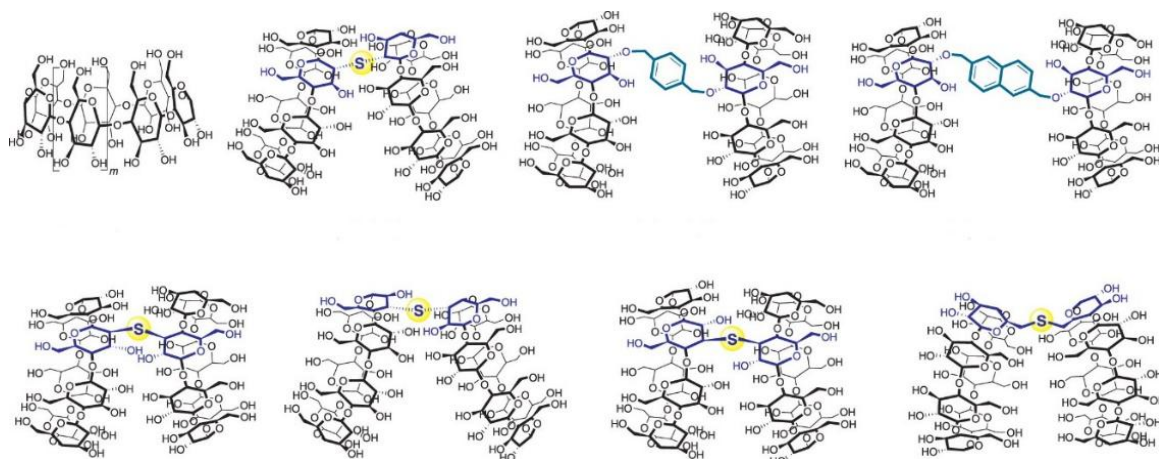


**Figure 2.16.** The structures of sulfur- and arene-linked cyclodextrin dimers and their stereoselectivity reported by Yang and co-workers.

An earlier case of synthesizing  $\beta$ -cyclodextrin dimers was reported by Williams and co-workers in 1997,<sup>34</sup> in which they afforded a series of linked cyclodextrins via the reactions of amino-substituted cyclodextrins with bis(3-nitrophenyl) oxalate, malonate, succinate and glutarate, and with diphenyl carbonate. Dimers linked by the primary or the secondary face of the  $\beta$ -cyclodextrin were prepared. The yields vary from 29% to 92% and the products are chemically stable. (Figure 2.17)

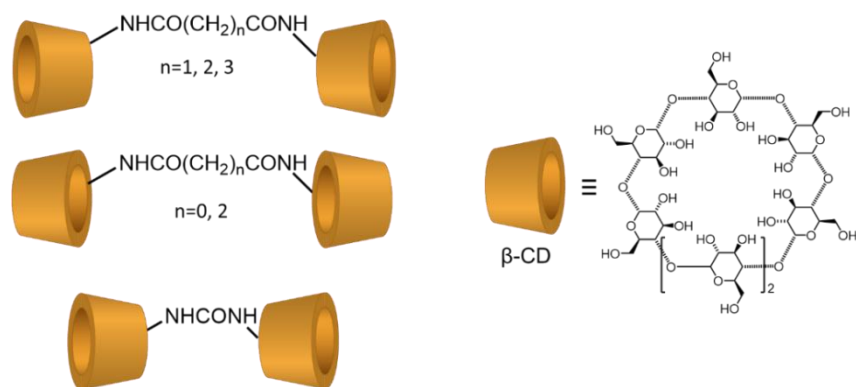


**Figure 2.17.** The structures of  $\beta$ -cyclodextrin dimers reported by Williams and co-workers.

### 2.3 Project Aims

This project aims are to synthesise a dimer of  $\beta$ -cyclodextrin in order to encapsulate 9-substituted barbaralanes so that their equilibrium distribution in the solid and in the solution state can be investigated in order to observe the noncovalent interactions. The 9-substituted barbaralanes possess a dynamic  $sp^3$  carbon stereocentre whose dynamics are similar to a rapidly transforming nitrogen center. By using covalent modifications as well as a macrocyclic host (such as chiral cyclodextrins) to create noncovalent interactions, the equilibrium distribution of barbaralanes stereoisomers in one of the two structures in solution and solid state could be controlled (Figure 2.3).

Previous research in McGonigal group, investigated two sets of nondegenerate fluxional barbaralanes, the parent barbaralol (**2.18**) and the tolyl-substituted barbaralol (**2.19**). The encapsulation and determination of binding stoichiometry were achieved by  $^1\text{H}$  NMR titrations as well as a single crystal. The results demonstrated that a 1:1 complex with the  $\beta$ -CD was formed in solution state as well as the solid state. The barbaralol (**2.18**) complex shows that the dynamic chirality is halted and pushed completely towards the S-enantiomer in the crystal structure (Figure 2.18), which suggests that the  $\beta$ -CD allows for noncovalent control over the fluxional  $sp^3$ -carbon stereocentre in the solid state.

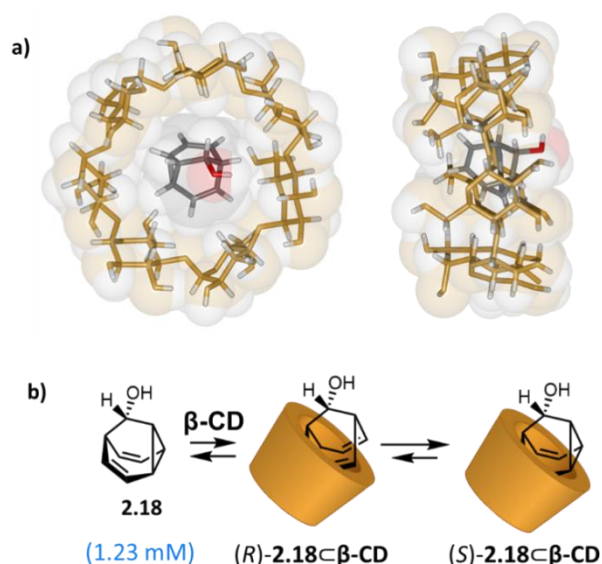


**Figure 2.18.** a) The crystal structure of **2.18** and  $\beta$ -CD complex and b) the effect of  $\beta$ -CD on the equilibrium distribution of **2.18** in the solid state.

However, for the complex of  $\beta$ -CD and the tolyl-substituted barbaralol (**2.19**), a head-to-head dimer is observed in the crystal structure, with one *R*- and one *S*-enantiomer in each  $\beta$ -CD cavity (Figure 2.19). This demonstrates a method racemic self-sorting in a homochiral environment – and is unexpected. In this project, we aim to further investigate the noncovalent control over  $sp^3$  carbon stereocentre, by synthesising a covalent-linked  $\beta$ -cyclodextrin dimer and using it to encapsulate the tolyl-substituted barbaralol to observe its effect on the dynamic chirality in solution and the solid state.

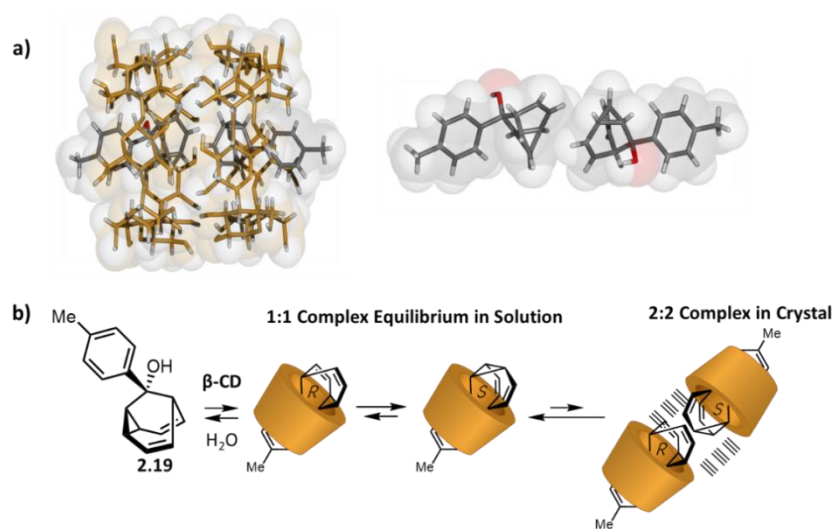
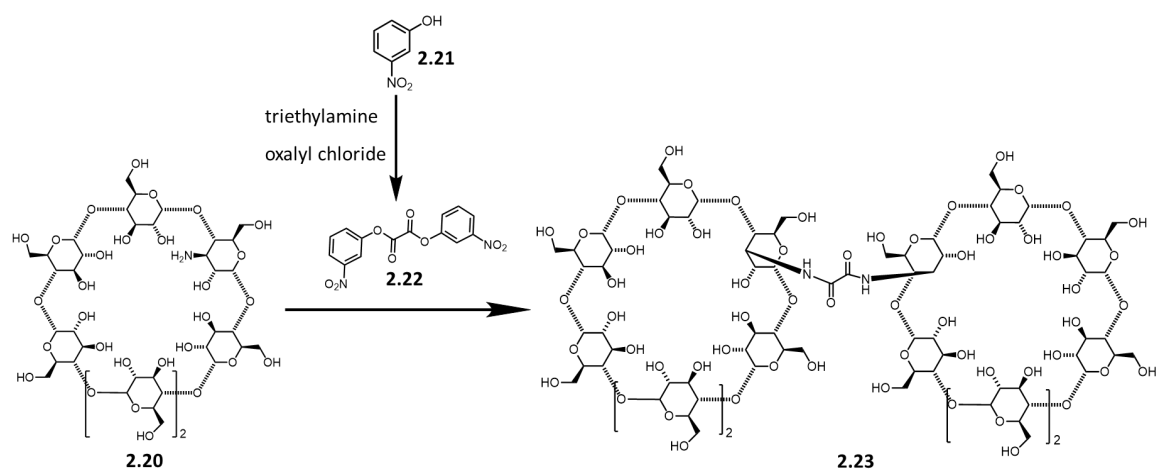


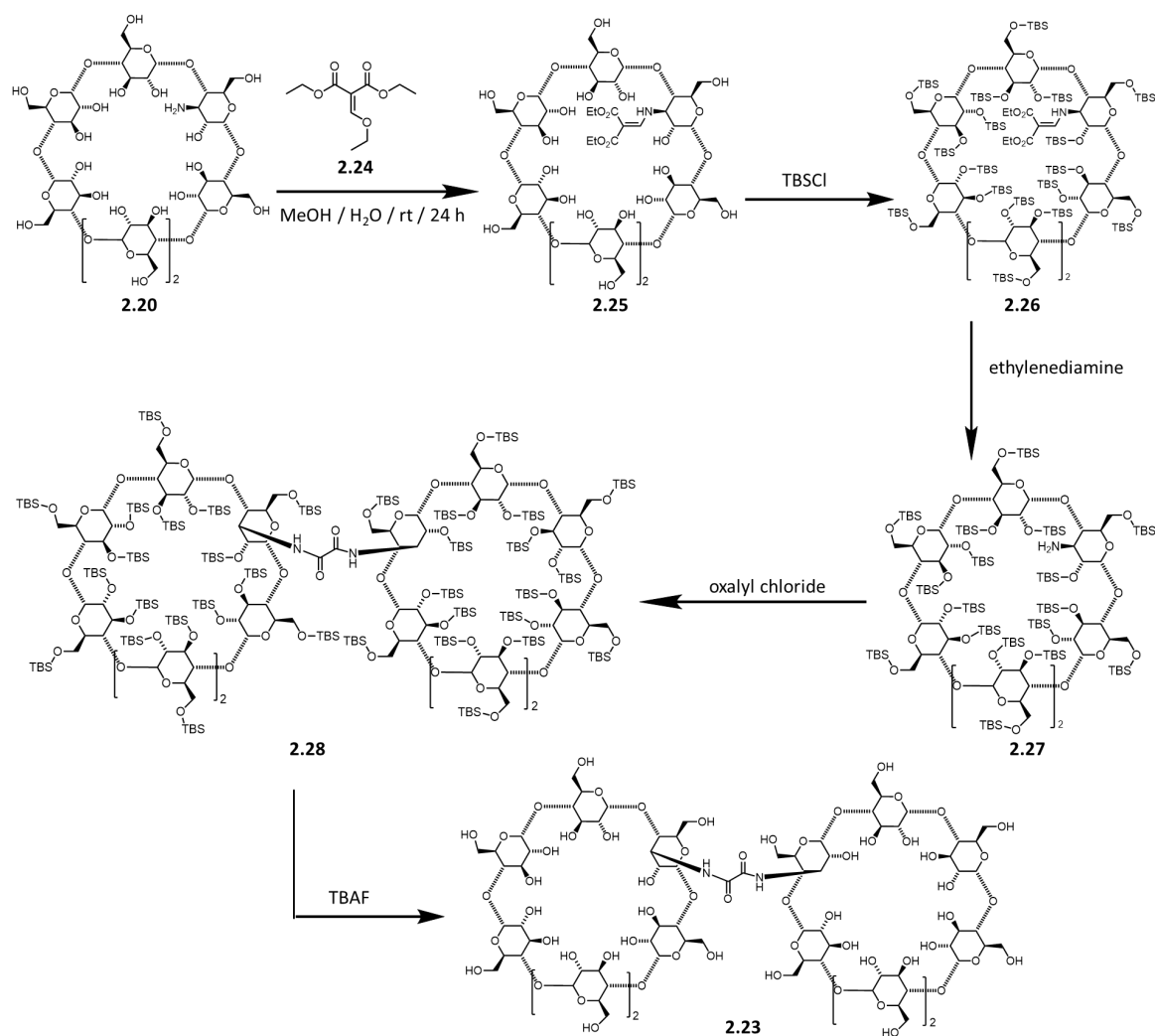
**Figure 2.19.** a) The crystal structure of **2.19** and  $\beta$ -CD complex. b) The effect of  $\beta$ -CD on the equilibrium distribution of **2.19** in the solid state.

For the design of the  $\beta$ -CD dimer **2.23**, we aim to follow the synthetic route reported by Williams to link the larger opening end of the two CD molecules via an oxalamide bond to imitate their relative position and distance in the 2:2 complex we observed in the solid state. A  $\beta$ -CD monomer **2.20** in which a hydroxyl group on the larger opening end is replaced by an amine group is selected as the substrate. Initially, we aimed to complete the synthesis of the dimer in two steps: The first step is to prepare a nitrophenol dimer **2.22** linked via an oxalic bond by the treatment of 3-nitrophenol **2.21** with oxalyl chloride and triethylamine, then **2.21** will work as the reagent to form the oxalamide linkage between two CD monomers. (Scheme 2.1)



**Scheme 2.1.** Initial synthetic route for  $\beta$ -CD dimer **2.23**.

However, the cyclodextrin is not soluble in an organic solvent and at the same time it is difficult to track the reaction process in practice. To solve this issue, the hydroxyl groups of the cyclodextrin should be all protected with *t*-butyldimethylsilyl (TBS) group, and the amine group should be protected in advance to avoid the reaction with the TBS reagent. As a result, when the hydroxyl groups are protected, we can simply use oxalyl chloride to form the oxalamide bond without preparing the nitrophenol dimer **2.22**. The complete revised synthetic route starts with the protection of the amine group with diethyl 2-(ethoxymethylene)malonate **2.24**, followed by the protection of the hydroxyl groups with *t*-butyldimethylsilyl chloride (TBSCl). Deprotection of the amine group occurs with ethylenediamine and the dimerization step uses oxalyl chloride. The finally step deprotects of the hydroxyl groups with tetrabutylammonium fluoride (TBAF) to get the desired dimer **2.23**. (Scheme 2.2)



**Scheme 2.2.** Revised synthetic route of  $\beta$ -CD dimer **2.23**.

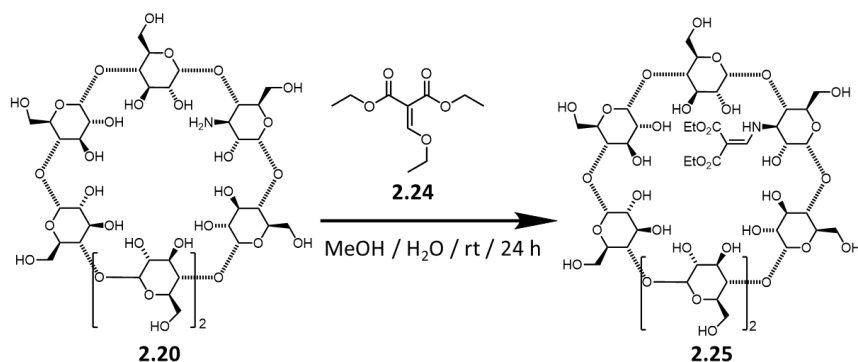
## 2.4 Results and Discussion

### Synthesis of bis(3-nitrophenyl) oxalate **2.22**

The reaction was carried under anhydrous conditions. The mixture of **2.23** and toluene was dried by azeotropic distillation. Triethylamine and oxalyl chloride were added under nitrogen and the reaction was kept under 10 °C (Scheme 2.3). The purification process was long and complicated including suction and recrystallization, as column chromatography could not be used due to the reactivity of the oxalate. The product **2.22** was obtained as yellow platelets in 4% yield, which is low but close to the literature data (6%).<sup>35</sup>



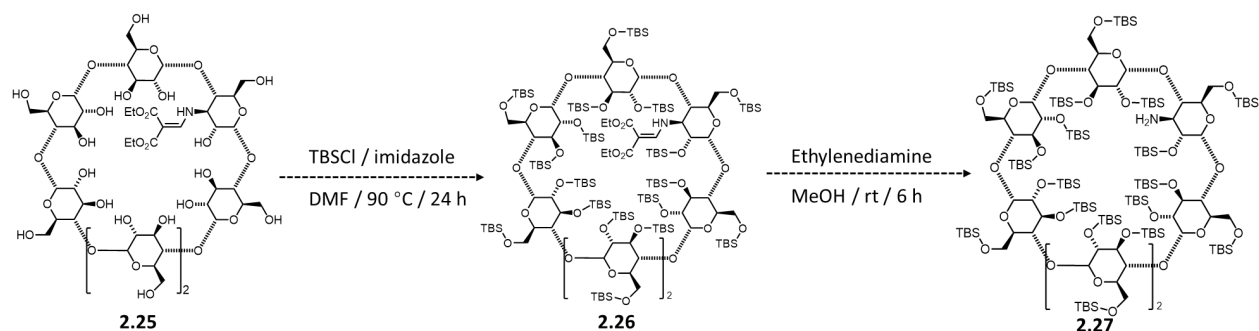
ppm) to all other hydrogen atoms except the exchangeable protons of hydroxyl groups (these range from 3.42 to 5.13 ppm) is 1:9, which is consistent with the molecular formula. This result was also confirmed by LC-MS:  $m/z = 1305.0152 [M+H]^+$ , which is consistent with the number calculated for  $C_{50}H_{82}NO_{38}^+$ : 1305.1667.



**Scheme 2.5.** Synthetic scheme of the amine group protection.

### Protection of the hydroxyl group and deprotection of the amine group

After protection of the amine group, **2.25** was treated with TBSCl and imidazole to protect all the hydroxy groups. Theoretically, the ratio of ethyl hydrogens on the protecting group (observed around 1.27 ppm) to all the hydrogen atoms on the TBS groups (around 0.08 and 0.88 ppm) should be 1:50. However, integrations of <sup>1</sup>H-NMR peaks indicated that this ratio in the product is only around 1:30. We still attempted to carry the obtained product onto the next step, and the integrations of NMR peaks were still incorrect, which indicated that the hydroxyl groups protection via TBSCl did not reach completion. The reason that the reaction did not work could be that TBS protection occurs readily on primary alcohols, but the secondary hydroxyl groups are hindered and too close in space to accommodate complete TBS protection. (Scheme 2.6)



**Scheme 2.6.** Failed attempts to synthesize **2.26** and **2.27**.

## 2.5 Conclusions and Future Work

The aim of this work has been to develop a  $\beta$ -cyclodextrin dimer in order to encapsulate the substituted barbaralanes and investigate noncovalent control over their dynamic equilibrium distribution in the solution and in the solid state. While synthesizing the  $\beta$ -cyclodextrin dimer, laboratory research was stopped due to the COVID-19 pandemic. Currently, only the amine protection has been completed, and currently the bottleneck is the TBS protection step. There is difficulty with this synthetic step and this could be due to the insensitivity of TBS reagent over secondary and tertiary alcohols. Due to this insensitivity, we plan to use a TMS reagent instead, as effective in the protection of carbohydrates. Once the hydroxyl groups are protected, the deprotection of amine group must occur and this will form the  $\beta$ -cyclodextrin dimer using ethylenediamine and oxalic acid, respectively.

After obtaining the  $\beta$ -cyclodextrin dimer, future work will look to titrate the dimer into a solution of the toyl-substituted barbaralol (**2.19**). NMR will be utilized to determine the binding constant. After the encapsulation, attempts will be made to obtain the crystal structure of the complex which will be determined by X-ray crystallography. The dynamic equilibrium of **2.19** under noncovalent control will be investigated and compared against the previous results of  $\beta$ -cyclodextrin monomer complex.

## 2.6 Experimental

### 2.6.1 General Methods

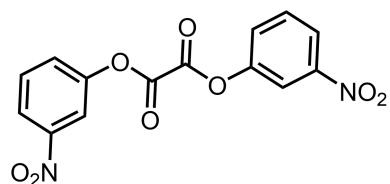
Unless otherwise stated, all reagents were purchased from commercial suppliers (Sigma-Aldrich, Fischer Scientific, or Tokyo Chemical Industry) and used without further purification. Air-sensitive reactions were carried out under a nitrogen atmosphere using Schlenk techniques. Purification by flash column chromatography was carried out using a Teledyne Isco CombiFlash Rf+ system, with pre-packed SiO<sub>2</sub> columns for the normal phase, and C18 columns for the reverse-phase chromatography, as the stationary phase.

Solution-phase NMR spectra were recorded using a Bruker Advance (III)-400 (<sup>1</sup>H 400.130 MHz and <sup>13</sup>C 100.613 MHz), Varian VNMRS-600 (<sup>1</sup>H 600.130 MHz and <sup>13</sup>C 150.903 MHz) or a Varian V-NMRS-700 (<sup>1</sup>H 700.130 MHz and <sup>13</sup>C 176.048 MHz) spectrometer, at a constant temperature of

298 K unless otherwise stated. Chemical shifts are reported in parts per million (ppm) relative to residual non-deuterated solvents [ $\text{CDCl}_3$ :  $\delta = 7.26$  or  $77.16$ .  $\text{D}_2\text{O}$ :  $\delta = 4.79$ ]. Coupling constants ( $J$ ) are reported in hertz (Hz). NMR spectra were processed using MestReNova version 12.0.3. Data are reported as follows: chemical shift, multiplicity, coupling constants, integration and assignment. Multiplicities are reported as singlet (s), doublet (d), triplet (t), and multiplet (m). High-resolution ESI-MS was performed using a Waters TQD UPLC ES MS/MS spectrometer.

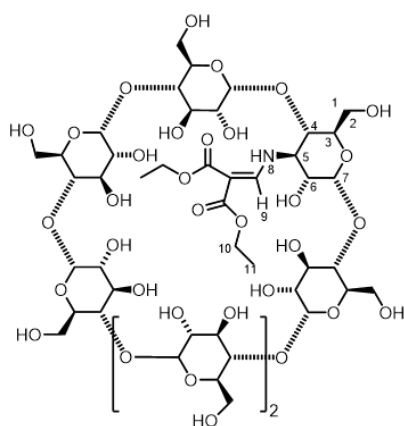
## 2.6.2 Synthetic Procedures

### Bis(3-nitrophenyl) oxalate 2.22



A solution of 3-nitrophenol (2.13 g, 15.3 mmol) in 40 ml of toluene was dried by azeotropic distillation. The solution was cooled to  $10\text{ }^\circ\text{C}$  under  $\text{N}_2$  atmosphere and triethylamine (2.1 g, 15.1 mmol) was added. Oxalyl chloride (0.64 ml, 7.5 mmol) was added with stirring; the temperature was kept below  $10\text{ }^\circ\text{C}$  using an ice bath. After 2 h stirring, a precipitate formed and was collected using Buchner filtration, following by drying under vacuum. The product was washed well with two 10 ml portions of dry chloroform to dissolve triethylammonium chloride and dried under vacuum. Recrystallization from acetonitrile afforded the title compound as pale yellow platelets (94.7 mg, 0.285 mmol, 4% yield).  $^1\text{H NMR}$  (400 MHz,  $\text{CDCl}_3$ )  $\delta$  8.26 (d,  $J = 7.9$  Hz, 1H), 8.22 (s, 1H), 7.70 (s, 1H), 7.67 (dd,  $J = 4.2, 2.4$  Hz, 2H). Characterization data are consistent with those reported previously: *Anal. Chim. Acta.* 1985, **177**, 103-110.

### Amine protection 2.25

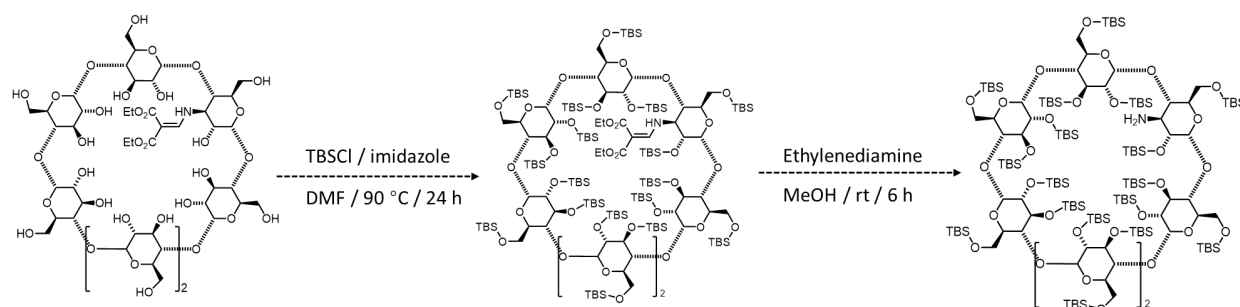


Amino-substituted cyclodextrin **2.20** (200 mg, 0.176 mmol) was dissolved in a 3:4 MeOH– $\text{H}_2\text{O}$  mixture (7 mL). Diethyl 2-(ethoxymethylene) malonate **2.21** (38 mg, 0.176 mmol) was added and the solution was stirred for 24 h at room temperature. The solvent was removed under reduced pressure, and the crude residue was purified via column

chromatography (Teledyne Isco CombiFlash Rf+ system, C18, H<sub>2</sub>O–MeOH gradient elution) to give the title compound **2.25** as a white solid (137 mg, 0.105 mmol, 59% yield). <sup>1</sup>H NMR (600 MHz, D<sub>2</sub>O): δ 1.30 (q, *J* = 8.6 Hz, 6H, H<sub>11</sub>), 5.13 - 5.02 (m, 7H, H<sub>7</sub>), 4.45 - 3.42 (m, 48H, H<sub>1/2/3/4/5/6/8/9/10</sub>). **HR-ESI MS**: *m/z* = 1305.0152 [M+H]<sup>+</sup>, calculated for C<sub>50</sub>H<sub>82</sub>NO<sub>38</sub><sup>+</sup>: 1305.1667.

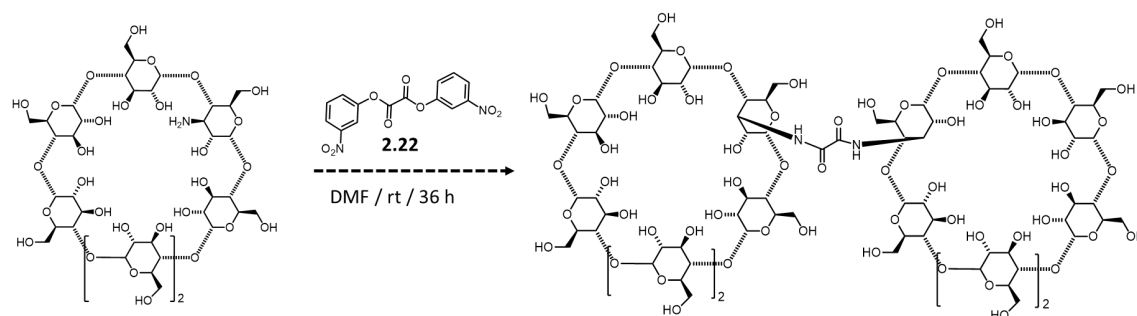
### 2.6.3 Failed reactions

#### TBS protection and amine deprotection:



Compound **2.22** (65 mg, 0.050 mmol) and imidazole (143 mg, 2.00 mmol) were dissolved in anhydrous DMF (5 mL). *t*-Butyldimethylsilyl chloride (158 mg, 1.00 mmol) was added into the mixture and the solution was reflux at 90 °C under N<sub>2</sub> for 24 h. The reaction solution was concentrated under reduced pressure, dissolved in CH<sub>2</sub>Cl<sub>2</sub> (20 mL), washed with water (10 mL) and purified *via* column chromatography (Teledyne Isco CombiFlash Rf+ system, 12 g SiO<sub>2</sub>, CH<sub>2</sub>Cl<sub>2</sub>-MeOH, gradient elution) to give the product as a brown-coloured solid (26 mg, 0.007 mmol). The product was dissolved in EtOH (3 mL), ethylenediamine (1.8 mg, 0.03 mmol) was added and the mixture was stirred at room temperature for 6 h. The solvent was removed under reduced pressure. The integration of the <sup>1</sup>H-NMR peaks was not as expected.

#### Dimerization of 2.20 by 2.22:



Bis(3-nitrophenyl) oxalate **2.22** (20 mg, 0.06 mmol) and amino-substituted cyclodextrin **2.20** (100 mg, 0.088 mmol) was dissolved in DMF (5 mL) and stirred at room temperature for 36 h. The solvent was removed under reduced pressure and the crude product was purified by reverse-phase column chromatography (Teledyne Isco CombiFlash Rf+ system, C18, H<sub>2</sub>O–MeOH gradient elution) to give the title compound as white solid. Characterization data is not able to be distinguished.

## **2.7 Appendices**

No additional information was required. All mass spectrometry data, NMR spectra and other analytical data can be found on the McGonigal group shared folder. (<\\prblue02.mds.ad.dur.ac.uk\vnvr72\PM\Yuzhen Wen>)

## 2.8 References

1. H. D. Flack, *Acta Cryst.* 2009, **A65**, 371 – 389.
2. N. H. Evans, *Chem. Eur. J.* 2018, **24**, 3101; J. C. Chambrom, C. Dietrich-Buchecker and J. P. Sauvage, *Top. Curr. Chem.* 1993, **165**, 131.
3. (a) S. Sugiyama, S. Wantabe, T. Inoue, R. Kurihara, T. Itou and K. Ishiii, *Tetrahedron.* 2003, **59**, 3417; (b) M. Alvarez-Pérez, S. M. Goldup, D. A. Leigh and A. M. Z. Slawin, *J. Am. Chem. Soc.* 2008, **130**, 1836.
4. B. Kim, G. Storch, G. Banerjee, B. Q. Mercado, J. Castillo-Lora, G. W. Brudvig, J. M. Mayer and S. J. Miller, *J. Am. Chem. Soc.* 2017, **139**, 15329.
5. (a) A. R. Lippert, A. Naganawa, V. L. Keleshian and J. W. Bode, *J. Am. Chem. Soc.* 2010, **132**, 15790; (b) K. Larson, M. He, J. F. Teichert, A. Naganawa and J. W. Bode, *Chem. Sci.* 2012, **3**, 1825; (c) J. F. Teichert, D. Mazunin and J. W. Bode, *J. Am. Chem. Soc.* 2013, **135**, 11314.
6. (a) J. G. Henkel and J. T. Hane, *J. Org. Chem.* 1983, **48**, 3858; (b) C. Engdahl and P. Ahlberg, *J. Am. Chem. Soc.* 1979, **101**, 3940; (c) L. G. Greifenstein, J. B. Lambert, M. J. Broadhurst, L. A. Paquette, *J. Org. Chem.* 1973, **38**, 1210; (d) G. G. Cristoph, S. Hardwick, U. Jacobsson Y.-B. Koh, R. Moerck and L. A. Paquette, *Tetrahedron. Lett.* 1977, **14**, 1249.
7. A. N. Bismillah, J. Sturala, B. M. Chapin, D. S. Yufit, P. Hodgkinson and P. R. McGonigal, *Chem. Sci.* 2018, **9**, 8631.
8. H. Jędrzejewska and A. Szumna, *Chem. Rev.* 2017, **6**, 4863 – 4899.
9. P. Timmerman, R. H. Vreekamp, R. Hulst, W. Verboom, D. N. Reinhoudt, K. Rissanen, K. A. Udachin and J. Ripmeester, *Eur. J.* 1997, **3**, 1823– 1832.
10. L. J. Prins, J. Huskens, F. de Jong, P. Timmerman and D. N. Reinhoudt, *Nature* 1999, **398**, 498-502.
11. W. Makiguchi, J. Tanabe, H. Yamada, H. Lida, D. Taura, N. Ousaka and E. Yashima, *Nat. Commun.* 2015, **6**, 7236.
12. P. N. Cheng, J. D. Pham and J. S. Nowick, *J. Am. Chem. Soc.* 2013, **135**, 5477-5492.
13. M. M. Safont-Sempere, P. Osswald, K. Radacki and F. Würthner, *Eur. J.* 2010, **16**, 7380- 7384.
14. A. M. Costero, M. Colera, P. Gaviña, S. Gil and L. E. Ochando, *J. Chem.* 2006, **30**, 1263- 1266.
15. J. M. Takacs, P. M. Hrvatin, J. M. Atkins, D. S. Reddy and J. L. Clark, *New J. Chem.* 2005, **29**, 263-265.
16. P. L. Arnold, J. C. Buffét, R. P. Blaudeck, S. Sujecki, A. J. Blake and C. Wilson, *Angew. Chem., Int. Ed.* 2008, **47**, 6033-6036.
17. M. Horie, N. Ousaka, D. Taura and E. Yashima, *Chem. Sci.* 2015, **6**, 714-723.

18. M. Mizumura, H. Shinokubo and A. Osuka, *Angew. Chem., Int. Ed.* 2008, **47**, 5378-5381
19. A. Villiers, *Compt. Rend.* 1891, **112**, 536.
20. Schardinger, *F. Wien. Klin. Wochenschr.* 1904, **17**, 207.
21. G. A. Hembury, V. V. Borovkov and Y. Inoue, *Chem. Rev.* 2008, **1**, 1-73.
22. W. L. Hinze, *Applications of Cyclodextrins in Chromatographic Separations and Purification Methods, Separation & Purification Reviews.* 1981, **10:2**, 159-237.
23. M. L. Bender and M. Komiyama, *Cyclodextrin Chemistry*, 1978, 19
24. H. Pringsheim, *Chemistry of the Saccharides*, 1932, 280.
25. G. Crini, *Chem. Rev.* 2014, **114**, 10940–10975
26. K. Harata, K. Uekama, M. Otagiri and F. Hirayama, *J. Incl. Phenom. Macro.* 1984, **2**, 583-594.
27. J. L. Jarman, W. J. Jones, L. A. Howell and A. W. Garrison, *J. Agric. Food Chem.* 2005, **53**, 16, 6175-6182.
28. (a) A. M. Stalcup and K. H. Gahm, *Anal. Chem.* 1996, **8**, 1369-1374; (b) P. Sun, A. Krishnan, A. Yadav, S. Singh, F. M. MacDonnell and D. W. Armstrong, *Inorg. Chem.* 2007, **24**, 10312-10320.
29. T. S. Straub and M. L. Bender, *J. Am. Chem. Soc.* 1972, **94**, 8881
30. D. L. Van der Jagt, F. L. Killian and M. L. Bender, *J. Am. Chem. Soc.* 1970, **92**, 1016.
31. (a) I. Ojima, *Catalytic Asymmetric Synthesis, 3rd ed.; John Wiley & Sons: Hoboken*, 2010; (b) R. Brimiouille, D. Lenhart, M. M. Maturi and T. Bach, *Angew. Chem., Int. Ed.* 2015, **54**, 3872; (c) E. Meggers, *Angew. Chem., Int. Ed.* 2017, **56**, 5668.
32. (a) P. Sun, A. Krishnan, A. Yadav, S. Singh, F. M. MacDonnell, and D. W. Armstrong, *Inorg. Chem.* 2007, **24**, 10312–10320; (b) B. Feibush, C. L. Woolley, and V. Mani, *Anal. Chem.* 1993, **9**, 1130–1133.
33. J. Ji, W. Wu, W. Liang, G. Cheng, R. Matsushita, Z. Yan, X. Wei, M. Rao, D. Yuan, G. Fukuhara, T. Mori, Y. Inoue and C. Yang, *J. Am. Chem. Soc.* 2019, **141**, 9225–9238.
34. C. J. Easton, S. J. van Eyk, S. F. Lincoln, B. L. May, J. Papageorgiou and M. L. Williams, *Aust. J. Chem.* 1997, **50**, 9-12.
35. K. Honda, K. Miyaguchi and K. Imai, *Anal. Chim. Acta.* 1985, **177**, 103-110.
36. A. N. Bismillah, PhD Thesis, Durham University, 2019.